Characterization of the Interaction of EEN and Its Domains with Ca^{2+} and Proline Rich Domain

ZHANG YUNING

A THESIS SUBMITTED TO THE DEPARTMENT OF BIOLOGICAL SCIENCE NATIONAL UNIVERSITY OF SINGAPORE FOR THE DEGREE OF MASTER OF SCIENCE

ACKNOWLEDGEMENT

I wish to express my gratitude to my supervisor, Dr Yang Daiwen, for his patient guidance, favourable advices and encouragement during the course of my work.

I am grateful to Dr Low and Dr Henry for the helpful discussions, comments and moral supports.

Lastly, I would like to thank all the members in my group for their constant support and kind help.

TABLE OF CONTENTS

LIST OF FIGURES

Figure

LIST OF TABLES

Table

ABSTRACT

EEN (Extra Eleven Nineteenth) is the human homology of Endophlin II and plays a crucial role in synaptic transmission and nervous system. EEN consists of 368 amino acids and exists as a dimer *in vitro*. According to secondary structure prediction and functions, EEN is divided into three domains: an alpha helical BAR (Bin/amphiphysin/Rvs) domain at C-terminus, a beta sheet SH3 (Src-homology-3) domain at N-terminus and a random coil domain between these two domains. To explore the possible role of this random coil domain, a polypeptide consisting of the SH3 domain and the random coil domain was designed and named as ΔBAR domain. The EEN full length, BAR domain, SH3 domain and ΔBAR domain were all cloned into pET-M, expressed in BL21(DE3) bacterial cell and purified with affinity and gel filtration columns. The interactions of Ca^{2+} and a peptide carrying the proline rich domain (PRD) with EEN and its three domains were investigated with NMR, ITC and other biochemical techniques. Our studies showed that Ca^{2+} has no influence on the structures of EEN, BAR domain and ΔBAR domain *in vitro*. In addition, the random coil domain does not affect the bridging of SH3 domain to PRD *in vitro*. Therefore, the random coil domain or Ca^{2+} is not involved in interactions between the EEN SH3 domain and PRD.

CHAPTER 1

INTRODUCTION

1.1 Motivation and objectives

Various studies on the Endophilin family of proteins suggest the crucial role of Endophilins in Clathrin-mediated endocytosis, which is essential in the synaptic vesicle (SV) recycling (Brodin et al., 2000; Gad et al., 2000; Huttner and Schmidt, 2002; Ringstad et al., 1999).

The C-terminal Src-homology-3 (SH3) domain of Endophlin selectively interacts with a few other endocytic proteins, such as dynamin and synaptojanin, via their proline-rich domain (PRD) (Reutens, 2002). On the other hand, its N-terminal BAR (Bin/amphiphysin/Rvs) domain is involved in binding or bending to the membranes for generating the curvature of the membranes (Farsad et al., 2001).

Endophilin also interact with the voltage-gated Ca^{2+} channels in a Ca^{2+} dependent manner (Chen et al., 2003). An interesting hypothesis was proposed suggesting that the SH3 domain of endophilin might bind to its own proline rich domain located between the SH3 domain and BAR domain in the presence of Ca^{2+} (Chen et al., 2003).

The proline-rich domain connecting the BAR domain and SH3 domain exists as a flexible random coil that allows both the BAR domain and SH3 domain to function separately. Up to date, there is no detail study on the role of this domain to the functions of the SH3 & BAR domains.

The praline-rich random coil domain exists in all the members of the Endophilin family but its amino acid sequence is not highly conserved as shown by BLAST analysis. An exception is that the PRD of Endophilin A2 that can interact with the Ca^{2+} channel always contain the canonical sequence 'PX+PX+' ("+" stands for negatively charged residue). The multiple negatively charged residues were believed to bind Ca^{2+} directly and play an important role in interaction with the Ca^{2+} channel (Chen et al., 2003).

The protein investigated in this study is the human homology of Endophilin A2, named as EEN (Extra Eleven Nineteenth) and consisted of 368 amino acids. In this work, a construct was designed to express just the random coil domain and the SH3 domain together which is named as the ΔBAR domain. The full-length protein and three constructs (BAR domain, SH3 domain and ΔBAR domain) were expressed and purified in several vector systems to study their interaction with Ca^{2+} as well as binding to PRD. The main objective of this study is to explore the

functional roles of the random coil PRD that connects the BAR and SH3 domains.

Several techniques were employed for both quantitative and qualitative studies of the structures and functions of the EEN and its three domains. Native PAGE, Circular Dichroism and NMR were used to exploit the interaction of Ca^{2+} with EEN and its domains. 2-D NMR and ITC were carried out to verify the binding between SH3 domain and the PRD as well as the influence of Ca^{2+} on this interaction.

1.2 Organization of the thesis

This thesis is divided into five chapters. In chapter 1, the motivation, scope and objectives of this research are explained, followed by the organization of the thesis. Chapter 2 gives a literature review on the subject matter of this study as well as the background for other research that had been done so far in this area. Chapter 3 describes the materials and methodology used in this work. In this chapter, the techniques of gene clone, protein expression and purification as well as the methods of chemical and physical studies on EEN and its domains are provided. Chapter 4 presents the results obtained, while Chapter 5 discusses the contribution of these results on understanding of the possible role of the

random coil PRD and the influence of Ca^{2+} on EEN *in vitro*. Chapter 6 concludes the finding of this research and gives future perspectives.

CHAPTER 2

Background and literature review

Endocytosis is a process in which a substance gains entry into a cell without passing through the cell membrane. Endocytosis results in the formation of an intracellular vesicle by virtue of the invagination of the plasma membrane and membrane fusion (Stahl et al., 2002). The process of receptor mediated endocytosis plays a very important role in human cholesterol metabolism. It is the major pathway by which cholesterol enters cells to be incorporated into cellular constituents or to be broken down and excreted (Goldstein et al., 1982). At the synapse, "clathrin-mediated endocytosis" is thought to be the major pathway by which vesicles are regenerated (Royle et al., 2003). The molecular mechanisms underlying clathrin-mediated endocytosis had been intensively studied (Slepnev and De Camilli, 2000; Royle et al., 2003).

Three main components involved in the clathrin-mediated endocytosis have been identified and studied, named as endophilin, dynamin and synaptojanin (Huttner and Schmidt, 2002; Slepnev and De Camilli, 2000). Among them, endophilin has been implicated in several stages of clathrin-mediated endocytosis (Gad et al., 2000; Song et al., 2003; Brodin et al., 2000). The removal of endophilin in Drosophila resulted in

blocking of clathrin-mediated endocytosis, which suggested that Endophilin is indispensable for the clathrin-mediated endocytosis (Verstreken et al., 2002). In addition, there is growing evidence linking the Endophilin family of proteins to non-endocytic functions.

The Endophilin A family has three members, which are Endophilin A1 (EA1), Endophilin A2 (EA2) and Endophlin A3 (EA3). These three proteins share approx. 70% identity but are distinct from each other in their biological functions and localizations.

EA1 localizes at the brain presynaptic nerve termini in brain. It forms a dimer similar to amphipysin through its N-terminus, and participates in multiple stages in clathrin-coated endocytosis, from early membrane invagination to synaptic vesicle uncoating. Both the N-terminal BAR domain and the C-terminal SH3 domain are required for endocytosis, the latter being involved in recruitment of synaptojanin and dynamin [Reutens et al., 2002; Szaszak et al., 2002]. Some non-endocytic proteins are also known to interact with the SH3 domain of EA1 based on yeast two-hybrid studies, including disin, a β1-adrenergic receptor and the metalloprotease tegrins [Tang et al., 1999].

Unlike the brain-specific EA1, EA2 is widely expressed in different tissues of the body (Ringstard et al., 2001). It has been shown to interact with Moloney-murine-leukaemia virus Gag protein and to modulate virion production (Wang et al., 2003). Recently people have identified a novel Endo2-binding partner, EBP (EEN-binding protein), which possesses inhibitory effects on Ras signalling and on cellular transformation induced by Ras (Yam et al., 2004).

EA3 is expressed preferentially in brain and testis and has been shown to co-localize and interact with Huntingtin protein in patients suffering from Huntington's disease to promote the formation of insoluble polyglutamine-containing aggregates (Sittler et al., 1998). EA3 can also recruit the mouse metastasis-associated protein 1 (Mta1) through its SH3 domain for regulation of endocytosis (Aramaki et al., 2005). Moreover, Endophilin A3 was found to form filamentous structures which could play a role in the structure integrity of microtubules (Hughes et al., 2004).

Besides these three members of Endophlin A, another group of Endophilins known as Endophilin B share similar structural and functional properties as members of Endophilin A. Endophilin B is distinct from Endophilin A. It is associated with intracellular membranes and does not appear to operate in endocytosis at the plasma membrane

(Karbowski et al., 2004). Endophilins B, like the Endophilins A, are highly conserved from yeast to humans.

The clathrin-mediated endocytosis is carried out by two separate functional domains in Endophilin. Its N-terminal BAR (Bin/amphiphysin/Rvs) domain is involved in binding or bending to the membranes which generates the curvature of the membranes (Farsad et al., 2001). BLAST searches with the sequence of Endophilin BAR domain revealed a large number of proteins, most of which were involved in intracellular transport especially endocytosis (Bianca et al., 2004). All these proteins including amphiphysins, sorting nexins (Snx), oligophrenins, centaurins, and arfaptins, belong to a family of Bin-Amphiphysin-Rvs (BAR) domain-containing proteins (Figure 1.1).

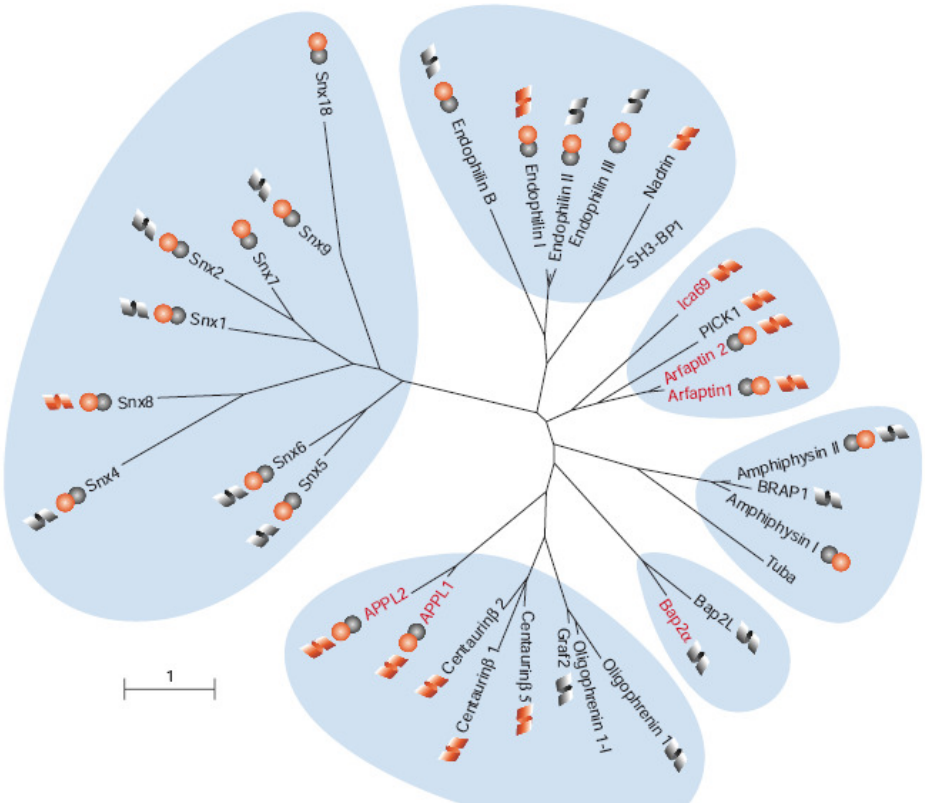

Figure 1.1 Phylogenetic Tree of proteins belonging to the BAR-domain family (Bianca et al., 2004).

The BAR domain consists of about 200 amino acids residues based on boundaries determined from sequence alignment. The domain displays a coiled-coil-like nature with a characteristic set of conserved hydrophobic, aromatic and hydrophilic amino acids. Although the sequence homology of BAR domains is low, e.g., the sequence homology between Amphiphysin and Endophlin 2 is only around 43%, they share similar functions as suggest by their similar structure (Zimmerberg et al., 2004).

The crystal structures of the BAR domain of Arfaptins and Amphiphysins, which share ~55% and ~43% homology respectively with the BAR domain of EEN, had been resolved recently and shown to be highly similar to each other. Both proteins form a crescent-shaped dimer composed of three helix coiled coil, despite of their highly distinct protein sequences (Bianca et al., 2004).

Based on stuctures of the Arfaptin 2 and the Amphiphysin BAR domain, it is believed that BAR-domain-containing proteins function as a dimmer and that formation of the dimer is dependent on their BAR domain. The Endophilin family is also found to form homo- or heterodimmers *in vivo* as a functional unit (Ringstad et al, 2001). Similarly, Arfaptin 2 itself forms a homodimer, which is a prerequisite for its binding to small GTPases (Tarricone et al, 2001). The V-shaped dimer of Amphiphysins may allow it to sense and/or induce membrane bending (Peter et al, 2003).

BAR-domain-containing proteins have been shown to bind to lipids and to bend membranes. The proposed model of BAR domain as a sensor of membrane curvature implies that the V-shaped structure of the dimer preferentially bended to curved rather than flat membranes (Huttner et al., 2002; Habermann et al., 2004).

Endophilin is the first family of proteins discovered to induce curvature in membrane (Takei et al., 1999). Initial work on Endophilin family suggested that a short stretch of sequence, adjacent to the amino (N)-terminus of the BAR domain is essential for lipid-binding and tubule formation by Endophilins (Farsad et al, 2001). This stretch of sequence at the N-terminal end is shown to form an amphipathic helix, thereby extending the helical backbone of the dimer at the tips. Together with the BAR domain, this sequence motif is termed as N-BAR and can be found in a subgroup of the BAR-domain containing proteins family, including Endophilins, Amphiphysins and Nadrin (Peter et al,2004).

Recently, the crystal structure of the endophilin A1 BAR domain had also been determined. The structure suggested that a new variant of BAR domain, which has an additional regulatory domain inserted at the concave side of the crescent-shaped dimer (Weissenhorn et al., 2005). The inserted domains might have additional membrane binding and sensing function, including the proposed lysophosphatidic acid acyl transferase activity (Schmidt et al., 1999).

On the other hand, its C-terminal Src-homology-3 (SH3) domain implies that Endophilin is a novel family of SH3 (Src homology region3) domain containing proteins. The SH3 domain of Endophlin-1 can interact with

the proline-rich domain (PRD) of synaptojanin, dynamin and other endocytic proteins (Ringstad et al., 1994; Simpson et al., 1999).

SH3 domain is a prominent feature of many signalling proteins and much work has been devoted to elucidating their binding specificity for proline-rich and other sequences. Peptide library studies have revealed that for many SH3 domains, recognition of 'PxxP' sequences is of low affinity (mid-high micromolar Kds) and specificity (Elena et al., 2005; Jack et al., 1998). High binding affinity of EEN SH3 domain requires a much elaborate sequence of "PPPXPP" (Ringstad et al., 2001). BPGAP1 is found to bind the SH3 domain of EEN in human and contains the sequence 'PPPXXPP' in its proline rich domain (Lua et al., 2005).

However, the recognition site for the Endophilin SH3 domain may be more complex than these motifs alone and could involve loops in the SH3 domain that interact with other elements of the specific proline rich domain.

Previous studies on Endophilin did not assign any function to the flexible domain connecting the BAR and SH3 domains. EEN contains a proline rich domain (PRD) at the flexible loop between BAR & SH3 domain, that feature the "PXXP" sequence motif and its function remains unclear.

The SH3 domain of EEN shares 55% identity with that of SEM-5 from *C.elegans*. The solution structure of the SH3 domain of SEM-5 was resolved by using NMR in 2003 and suggested a flexible beta-sheet structure (Ferreon et al., 2003).

Interestingly, Endophlilin was found to form a complex with the Ca^{2+} channel, which is essential for the clathrin-madiated synaptic vesical endocytosis (Chen et al., 2003). The author have suggested a molecular model for the Ca^{2+} dependent interaction between Endophilin and Ca^{2+} channels in which Endophilin is required for Ca^{2+} binding.

A hypothesis was proposed for the probable interaction between the SH3 domain and the intramolecular prolin rich domain which is located at the random coil domain between the BAR and SH3 domains of Endophlilin A2. This interaction might be stimulated by Ca^{2+} binding at the negatively charged residue adjacent to the proline rich domain (Figure 1.2).

Although both the Bar and the SH3 domains of Endophilin have been extensively studied for years, the function of the random coil part that connects these two domains remains unclear. The hypothesis suggested a

potentially very important role for this region of Endophilin when it coordinates with the Ca^{2+} channel for synaptical recycling.

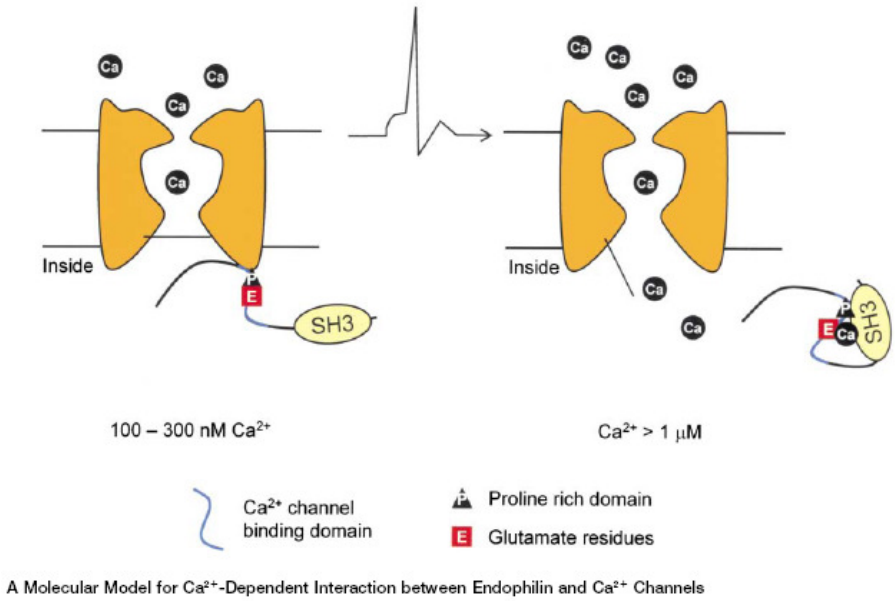

Figure 1.2 A Molecular model for Ca^{2+} -dependent interaction between Endophilin and Ca^{2+} channels (Chen et al., 2003).

In this work, the human homologue of Endophilin A2, EEN (extra eleven nineteen), is chosen as the study object. EEN is ubiquitously expressed in human and known as a binding partner for the MLL (mixed-lineage leukaemia) protein. Its gene was found to locate on chromosome 19p13 where two other MLL partner genes, ENL and ELL/MEN, had also been identified (So et al., 1997).

The full length EEN and its three domains (BAR domain, ΔBAR domain and SH3 domain) were expressed in BL21 bacterial system. The Ca^{2+} binding abilities of EEN and ΔBAR domain were studied *in vitro.* The interference of the random coil domain on the interaction between SH3 domain and the PRD *in vitro* was also studied in detail to determine the potential function of this random coil domain of EEN.

CHAPTER 3

MATERIALS AND METHODOLOGY

3.1 Clone of recombinant protein

3.1.1 Vector Design

To minimize the size of the vector, pET-32a (+) (maps and sequence landmarks were shown in figure3.1 and table3.1) was truncated to fit for the requirement. The truncated vector was named as pET-M.

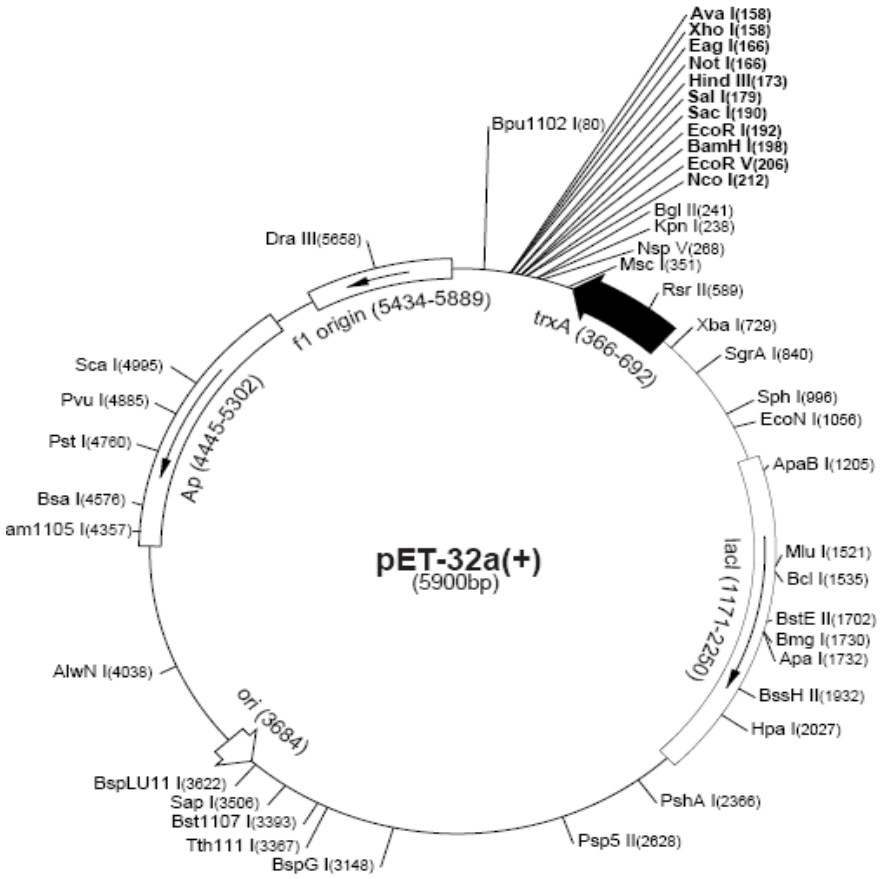

Figure 3.1: Map for pET-32a (+): the pET-32 series is designed for cloning and high-level expression of peptide sequences fused with the 109aa Trx.Tag ^{TM} thioredoxin protein.

T7 promoter	764-780
T7 transcription start	763
Trx•Tag coding sequence	366-692
His•Tag coding sequence	327-344
S•Tag coding sequence	49-293
Multiple cloning sites(*Nco* I – *Xho* I)	158-217
His•Tag coding sequence	140-157
T7 terminator	26-72
lacI coding sequence	1171-2250
pBR322 origin	3684
bla coding sequence	4445-5302
F1 origin	5434-5889

Table 3.1: pET-32a (+) sequence land marks.

pET-M was obtained after deleting the Trx.Tag coding sequence and S.Tag coding sequence from pET-32a(+). The BamH1 cutting site was also engineered to combine with the thrombin cutting site at the C-terminal Gly & Ser residues.

All the fusion proteins expressed in pET-M contained a His-tag and a Thrombin cutting side at the N-terminal region with the following sequence:

5'- M H H H H H H S S G L V P A G S A M A D I G S -3'

Two extra amino acids (Gly & Ser) residue will remain at the N-teminal of the protein after removal of the His-tag by thrombin digestion.

3.1.2 Cloning of EEN full length and its domains

The EEN full length DNA was amplified by PCR from an EEN-Flag plasmid obtained from Dr.Low(NUS) using a pair of primers named as EENFL BamH1 forward and EENFL XhoI reverse. Thereby, the BamH1 and XhoI restriction sites were introduced at the N-terminal and C-terminal of EEN respectively. The EEN DNA as well as the pET-M vector was cleaved with BamH1 and Xho1 and ligation was performed at 20°C overnight. The resulted plasmid was named N-terminal $(His)_6$-tag-EEN Full length.

EEN BAR domain, SH3 domain and ΔBar domain were also cloned follow the conditions above.

3.1.3 SH3p11 cloning system

Because there is one XhoI restriction site at the middle of the SH3p11 gene, the SH3p11 was cloned into pETM using *BamH1* and *EcoR1* restriction sites.

Using the rat liver cDNA as a template, the sh3p11 was cloned by the following 2-step PCR procedure:

First-step PCR procedure:

1 X	94°C		4 mins
30 X		94°C	30s
		62°C	30s
		72°C	70s
1 X	72°C		10mins
1 X	4°C		∞

Second-step PCR procedure:

1 X	94°C		4 mins
30 X		94°C	30s
		58°C	30s
		72°C	70s
1 X	72°C		10mins
1 X	4°C		∞

The 50µl PCR system was as following:

Template (rat CDNA/ first PCR product):	2µl
Forward primer (10µM)	5µl
Reverse primer (10µM)	5µl
dNTP	1µl

10 X Tag buffer	5µl
Mg^{2+}	3µl
H_2O	29µl

All final constructs were confirmed by sequencing.

3.2 Expression of EEN and its domains

Plasmids encoding these constructs were transformed into *E. coli* strain BL21 (DE3). After growing to an appropriate optical density at 37°C, protein expression was induced by the addition of 1M IPTG to a final concentration of 0.1mM IPTG and continue shaking at 20°C for overnight (15-18hours). All the cultures except for the EEN Full Length, BAR domain as well as SH3p11 were shaken at the speed of 180 rpm, while the EEN FL, BAR domain and SH3p11 were both shaken at the speed of 100rpm for lower self-aggregation rate.

3.3 Purification of EEN and its domains

The cultures of EEN and its domains were processed for protein purification by affinity chromatography. Briefly, bacterial pellets were firstly stored at -80°C for two hours, then were sonicated in 1 X PBS,

1mM DTT every other one minutes for 8 to 10 times, the one minutes intermission was for cooling down the solution. The sonicated solution was subjected to centrifugation at 25,000 rpm for 30 minutes. Pellet and supernatant were stored separately for future usage.

The supernatant was directly loaded onto a Ni-NTA affinity column (Ni-NTA Agarose was bought from QIAGEN). The column was rotated slowly at 4°c for 2 hours to let the protein fully bind to the beads. Then the beads was sequentially washed with 8 bed volumes each of 20 mM Tris, pH 8.0, 0.25 mM NaCl and 20 mM Tris, pH 8.0, 0.25 mM NaCl ,10 mM imidazole. Bound protein was then eluted with 0.25 M imidazole, 0.5 M NaCl, 0.02M Tris pH 8.0. The eluted protein was then dialysed against 1X PBS 1mM DTT buffer at 4°c.

Thrombin (Amersham Biosciences) was added depending on the estimated concentration of protein and the reaction was incubated at room temperature for 1.5 hours.

Then the Fast protein liquid chromatography (FPLC) was used to purify the protein further and eliminated the thrombin as well. FPLC was performed at Hiload 16/60, Superdex 75 pep grade from Amersham

Pharmacia biotech. The balance volume was 180mL, and the running speed was set at 0.5ml/min during every running.

3.4 Cloning, expression and purification of Proline rich domain of BPGAP1 (BPGAP1-PRD)

Sequence was choose by a cordon chart suggesting the most suitable cordon for Escherichia coli (Toshimichi et al., 1985)

The cordon is as following:

5'- ACC AAA ACC CCG CCG CCG CGT CCG CCG CTG CCG ACC CAG-3'

Reverse primer and forward primer were designed also for PCR:

Forward primer:

5'- C GCG GGA TCC ATG ACC AAA ACC CCG CCG CCG -3'

Reverse primer:

5'- C GCG CTC GAG TCACTG GGT CGG CAG CGG CGG -3'

The PRD plasmid was extracted after using one step PCR as following:

1 X 94°C 4 mins

30 X		94°C	30s
		50°C	30s
		60°C	10s
1 X 72°C			10mins
1 X 4°C			∞

PEGX4T1 was taken as the vector to get a GST fusion peptide construct. The Proline rich domain of BPGAP1 was expressed in BL21DE3 system. After shaking at 37°C for 2 hours, it was induced with 0.5mM IPTG for 5 hours at the same temperature.

Glutathione affinity column (Glutathione Sepharose 4B was bought from Amersham Biosciences) and HPLC were used for the purification of BPGAP1-PRD peptide.

3.5 NMR study on EEN

All the NMR spectra were obtained from an 800MHz Bruker Avane NMR performed at 298K.

3.6 Binding affinity study using ITC

The Isothermal Titration Calorimeter (ITC) was used to obtain the Calorie released spectrum when SH3 domain of EEN binding to the

peptide of the PRD of BPGAP1 (VP-ITC was made from MictroCal). The peptide was prepared as 1M for 300 μl, and the SH3 domain and ΔBAR domain of EEN was prepared as 0.05M for 1.2ml, the test was performed at 25ºC. The software Origin 7.0 was then used to fitting the titration curve and calculating the Kd value.

CHAPTER 4

RESULTS

4.1 EEN full length purification and Ca^{2+} binding study

```
      1          11         21         31         41         51
      |          |          |          |          |          |
    1 MSVAGLKKQF YKASQLVSEK VGGAEGTKLD DDFKEMEKKV DVTSKAVTEV LARTIEYLQP

   61 NPASRAKLTM LNTVSKIRGQ VKNPGYPQSE GLLGECMIRH GKELGGESNF GDALLDAGES

  121 MKRLAEVKDS LDIEVKQNFI DPLQNLCEKD LKEIQHHLKK LEGRRLDFDY KKKRQGKIPD

  181 EELRQALEKF EESKEVAETS MHNLLETDIE QVSQLSALVD AQLDYHRQAV QILDELAEKL

  241 KRRMREASSR PKREYKPKPR EPFDLGEPEQ SNGGFPCTTA PKIAASSSFR SSDKPIRTPS

  301 RSMPPLDQPS CKALYDFEPE NDGELGFHEG DVITLTNQID ENWYEGMLDG QSGFFPLSYV

  361 EVLVPLPQ
```

Table 4.1.1: Amino acids sequence of EEN. BAR domain was shown in red colour; SH3 domain was shown in green colour; black colour letters represented the random coil connecting the SH3 domain and the BAR domain of EEN.

EEN contains 368 amino acids, which consists of SH3 domain and BAR domain (Table 4.1.1). It was over-expressed in BL21 DE3, which was induced at 20 degree overnight (Figure 4.1.1).

The molecular weight of EEN monomer is about 42 kDa, however, the FPLC result suggested EEN existed as a dimer *in vitro*(Figure 4.1.2), and it was coincident with the existence of endophilin dimer *in vivo* at the nerve system synapses (Ringstad et al, 2001).

Nonetheless, the EEN full length was very unstable in the 1 X PBS buffer with 1mMDTT. The stability test suggested that 0.1mM EEN in solution would form white precipitate after 12 hours at 4°C or 5 hours at 37°C. An increase of salt concentration from 0 to 500mM or pH value from 6.0 to 8.0 could not prevent the aggregation. In addition, the method of using 100mM Glu+Arg to improve the solubility and stability of the protein was attempted (Alexender et al., 2004). But the FPLC elution and the profile Native PAGE result suggested no improvement on the purity and stability of EEN.

Native PAGE results suggested that there were also some tetramers and polymers which can not be separated from the dimer by the FPLC because of the large molecular weight (Figure 4.1.3). In further, these polymers may accelerate the process of the EEN aggregation. Therefore preventing the formation of the polymers during expression was necessary to stop the EEN self-aggregation *in vitro*.

A.

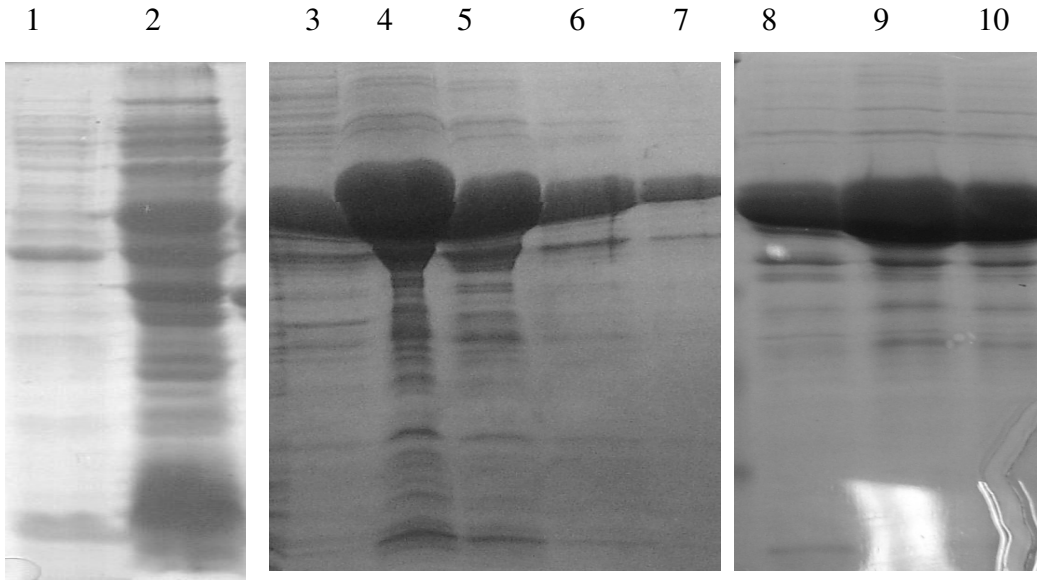

Figure 4.1.1 A: SDS-PAGE study on EEN full length. Lane 1: wash through of Ni-NTA affinity column; lane 2: flow through of Ni-NTA affinity column; Lane 3-7: elution with 1, 2, 3, 4, 5 times of bed volume separately; lane 8-10: the three samples collected at the centre of the main peak of FPLC from left to right.

B.

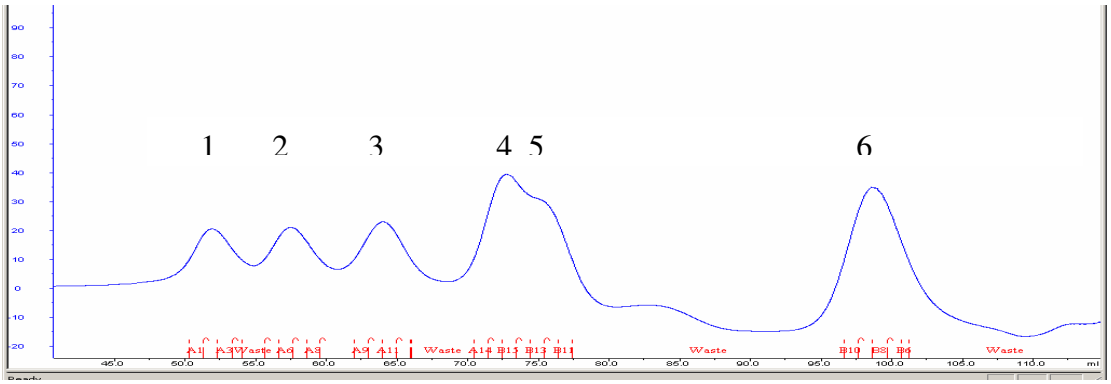

Figure 4.1.1 B: Standard chart of FPLC UV Spectrum of protein marker. Peak1: 93 kDa; Peak2: 50 kDa; Peak3: 35 kDa; Peak4: 28 kDa; Peak5: 21 kDa; Peak6: a fake peak which containing no protein proved by SDS PAGE.

C.

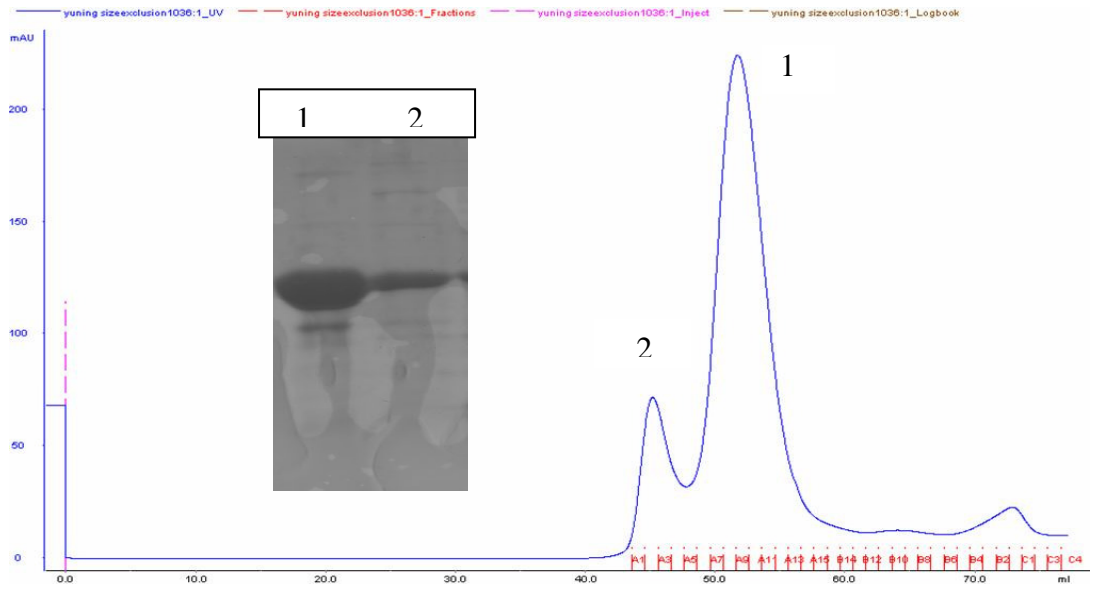

Figure 4.1.1 C: FPLC UV spectrum of EEN full length shaking under 100 rpm during expression. The picture on the left is the SDS PAGE of the EEN full length. Lane 1: the main peak of the FPLC; Lane 2: the first peak supposed to be the polymer of very high molecular weight.

D.

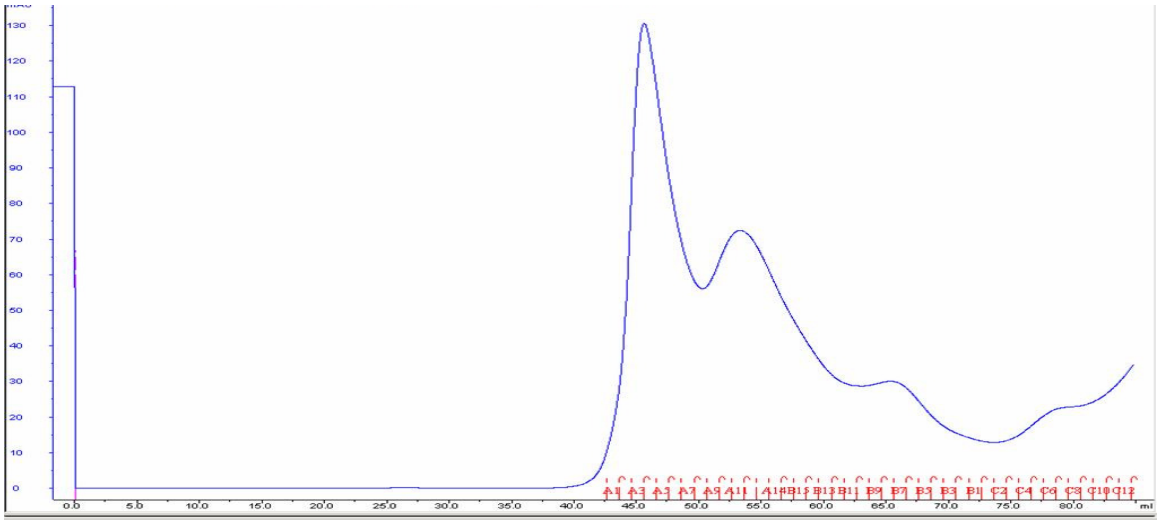

Figure 4.1.1 D: FPLC result of EEN full length (shaking speed over 100 rpm during expression).

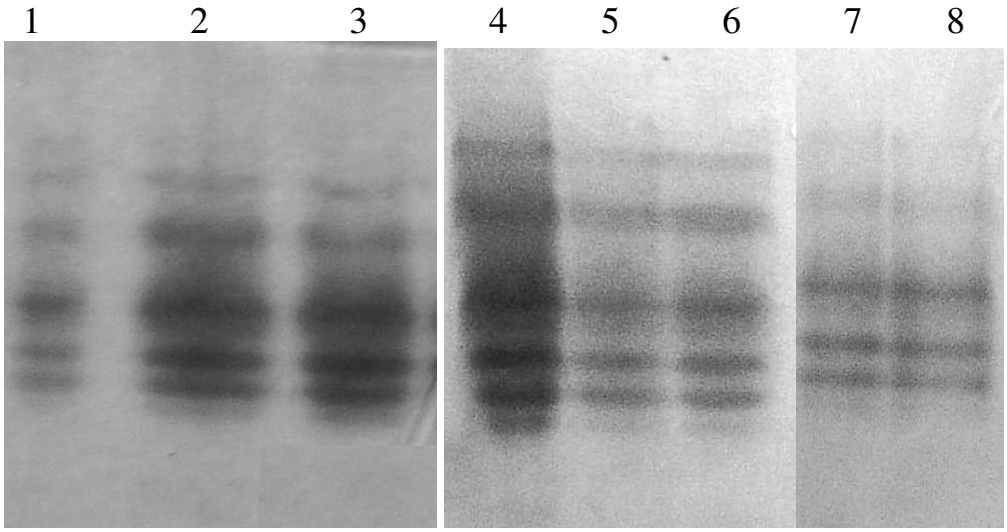

Figure 4.1.2 Native PAGE of EEN full length in different buffers. Lane 1: control EEN in 1XPBS, 1mMDTT; lane2: EEN in 5μM EDTA, 1XPBS, 1mM DTT; lane3: EEN in 10μM EDTA 1XPBS, 1mM DTT; lane 4, 5, 6: EEN in 15μM Ca^{2+}, 10μM Ca^{2+}, 5μM Ca^{2+} respectively; Lane7: add 10μM EDTA in lane 4; lane 8: add 10μM EGTA in lane 4.

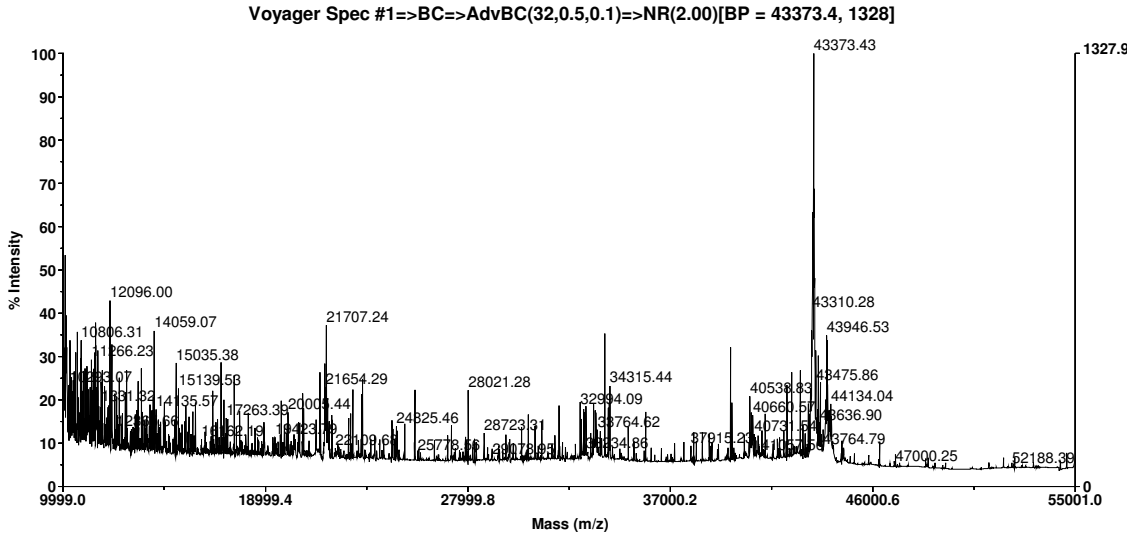

Figure 4.1.3 The Multi-TOF Mass Speculum of EEN full length, main peak suggested a 43.373 kDa protein while the theory molecular weight of EEN full length was 43.35 kDa.

An interesting difference on the aggregation state of EEN at different shaking speed was found during the expression of EEN in BL21. The aggregation problem was highly improved when the shaking speed was reduced from 180 rpm to 100 rpm as observed from the FPLC elution profile of full length EEN. Further reduction of the shaking speed made no difference on the extent of self-aggregation (Figure 4.1). This result also suggested that the aggregation started even at expression rather than during purification. On the other hand, an increase in the concentration of DTT did not help to prevent the EEN from self-aggregation. This might suggest that the four cystines in the sequence did not play a major role on the self aggregation of EEN.

The CD spectrum of EEN suggested alpha helical structure was dominated in the dimer of EEN (Figure 4.1.4). However both the CD spectrum and native PAGE results remain unchanged when the concentration of Ca^{2+} was increased (Figure 4.1.2). Also, 1-D NMR suggests no difference at different Ca^{2+} concentrations (data not shown here). Based on these results, Ca^{2+} does not bind EEN *in vitro*.

Figure 4.1.4 Circular diagram of EEN full length, scanning from 195nm to 250nm.

4.2 Cloning, expression and purification of BAR domain

Based on sequence alignment, the N-terminal 243 amino acids of EEN consists of a BAR domain. The molecular weight of BAR domain is about 29 kDa, while it was also found that BAR domain existed as a dimer in 1XPBS, 1mM DTT from the result of the FPLC (Figure 4.2.1 A and B). It was also consistent with the X-ray structure of the dimeric BAR domain of Endophlin-1 and Amphiphysin (Weissenhorn et al., 2005; Brain et al., 2004).

The solubility and stability of BAR domain were similar to those of full length EEN. Visible white precipitate was observable shown from a solution of 0.1 mM BAR domain after 2 days at 4ºC. Increasing of salt concentration from 0 to 500mM or pH value from 6.0 to 8.0 did not improve solubility of the BAR domain. Multi-TOF Mass spectrum of BAR domain also suggested certain degree of degradation after storage at room temperature for a week (Figure 4.2.2).

The CD spectrum suggested an alpha helical structure of the BAR domain dimer *in vitro* (Figure 4.2.3).

Although BLAST sequence search of BAR domain shown a low sequence homology among members in the family of Bin-Amphiphysin-Rvs (BAR) domain-containing proteins, which includes amphiphysins, sorting nexins (Snx), oligophrenins, centaurins, and arfaptins, their BAR domains share similar structures based on available structures and secondary structure prediction (Figure 4.2.4).

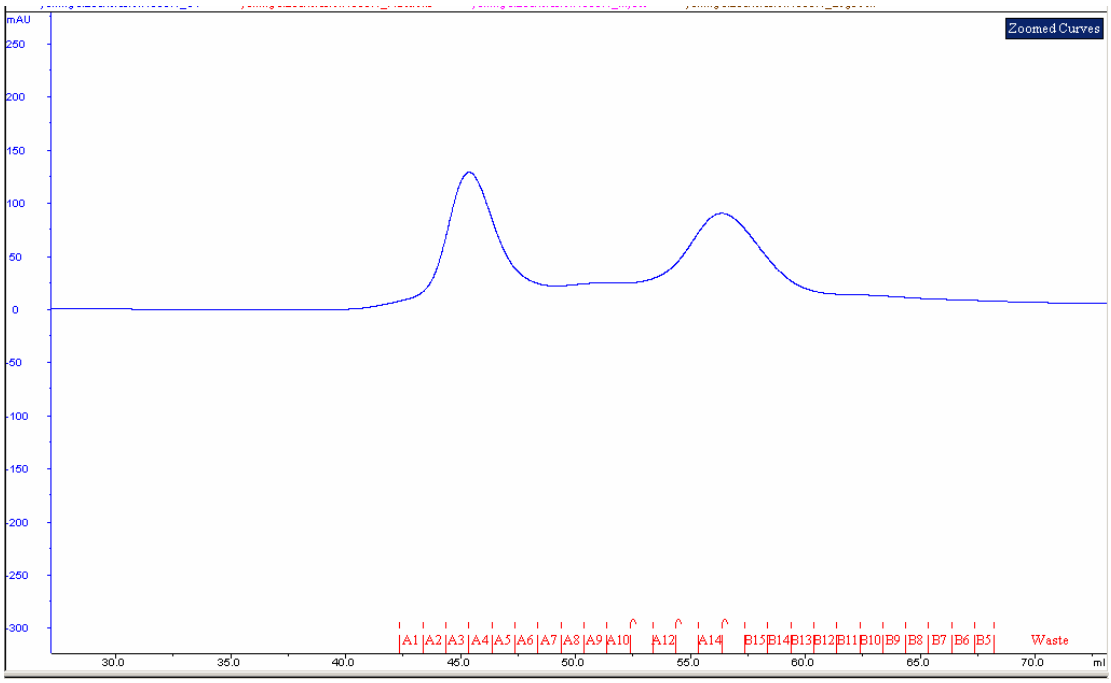

Figure 4.2.1 A: FPLC UV Spectrum of BAR domain of EEN.

B.

1 2

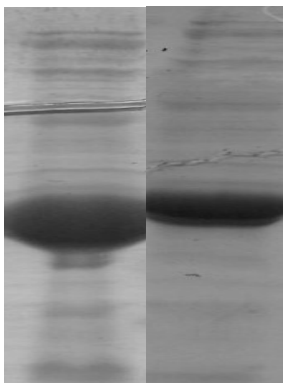

Figure 4.2.1 B: SDS PAGE of BAR domain of EEN after FPLC purification. Picture 1 stands for the first major peak in FPLC; picture 2 stands for the second major peak in FPLC

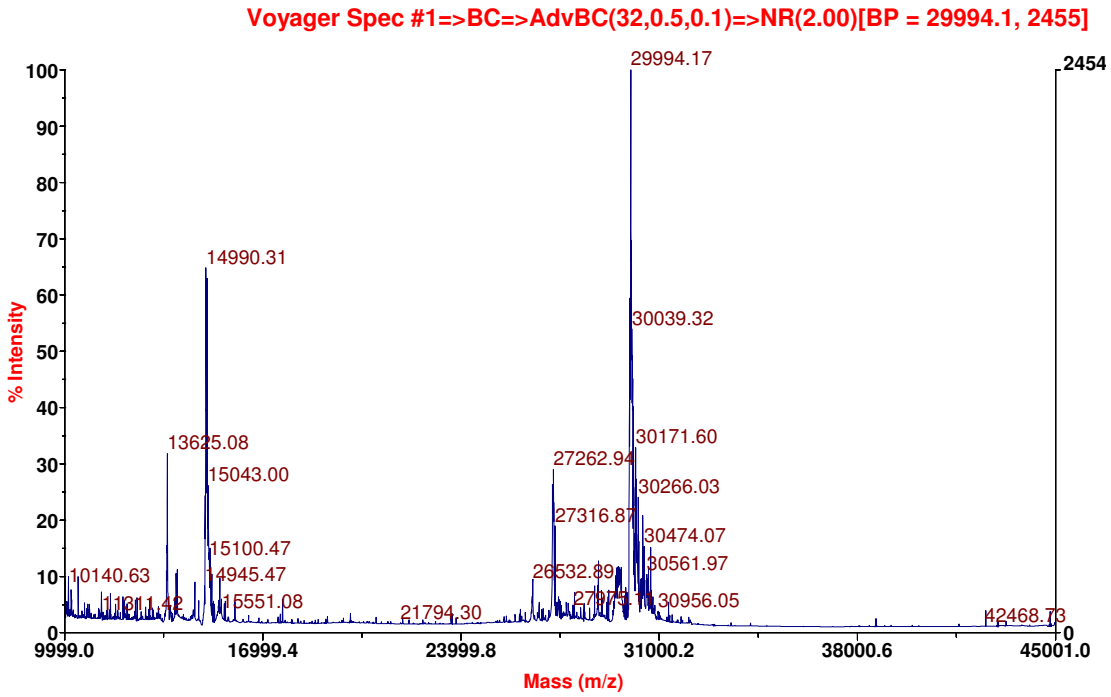

Figure 4.2.2 Multi TOF MS of BAR domain.

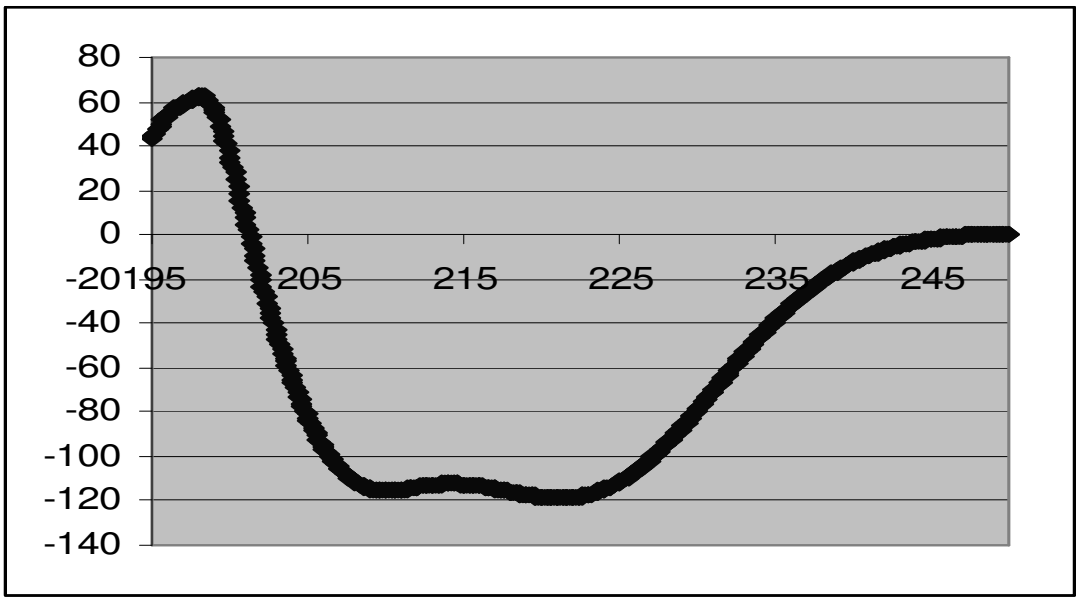

Figure 4.2.3 CD spectrum of BAR domain of EEN scanning from 190nm to 250 nm.

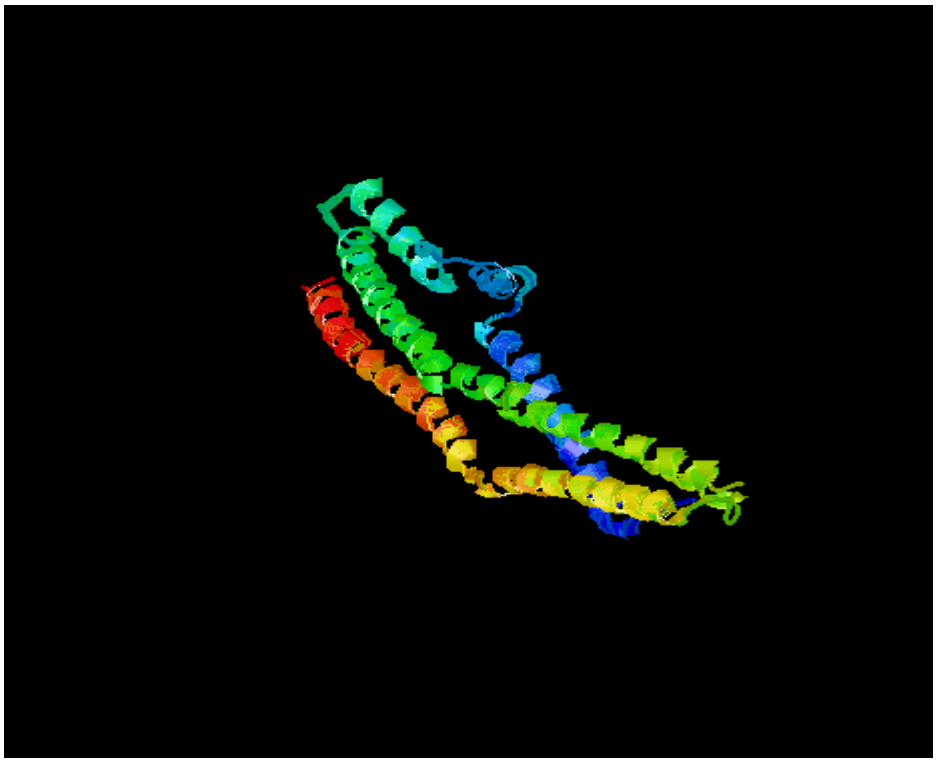

Figure 4.2.4 Secondary structure prediction of BAR domain of EEN using SWISS-MODEL.

4.3 purification and Ca^{2+} binding ability study of ΔBAR domain

To explore the possible functions of the random coil domain, which connects the SH3 domain with the N-terminal BAR domain of EEN, the random coil domain was cloned and expressed. Unfortunately, the purified protein was not stable and most of the protein was self-aggregated (Figure 4.3.1).

```
      1          11         21         31         41         51
      |          |          |          |          |          |
    1 MREASSRPKR EYKPKPREPF DLGEPEQSNG GFPCTTAPKI AASSSFRSSD KPIRTPSRSM

   61 PPLDQPSCKA LYDFEPENDG ELGFHEGDVI TLTNQIDENW YEGMLDGQSG FFPLSYVEVL

  121 VPLPQ
```

Table 4.3.1 amino acids sequence of ΔBAR domain of EEN. Green letters stands for the SH3 domain; Black letters stands for the random coil domain.

The ΔBar domain which consists of the SH3 domain and the random coil to determine the foundational roles of the random coil was designed (Table 4.3.1)

The expression level of ΔBar was very high in BL21 (DE3), and no large scale self-aggregation was observed during purification (Figure 4.3.2). Interestingly, when expressed in 1 X LB, there were two bands shown in SDS PAGE after purification (Figure 4.3.3 A:). Only a single band was observed when expression was done in 1 X M9 (Figure 4.3.3 B:). However, from the analysis of the spectrum of 1-D NMR spectrums and the results of the FPLC, it was believed that EEN ΔBar existed mainly as a monomer (Figure 4.3.4).

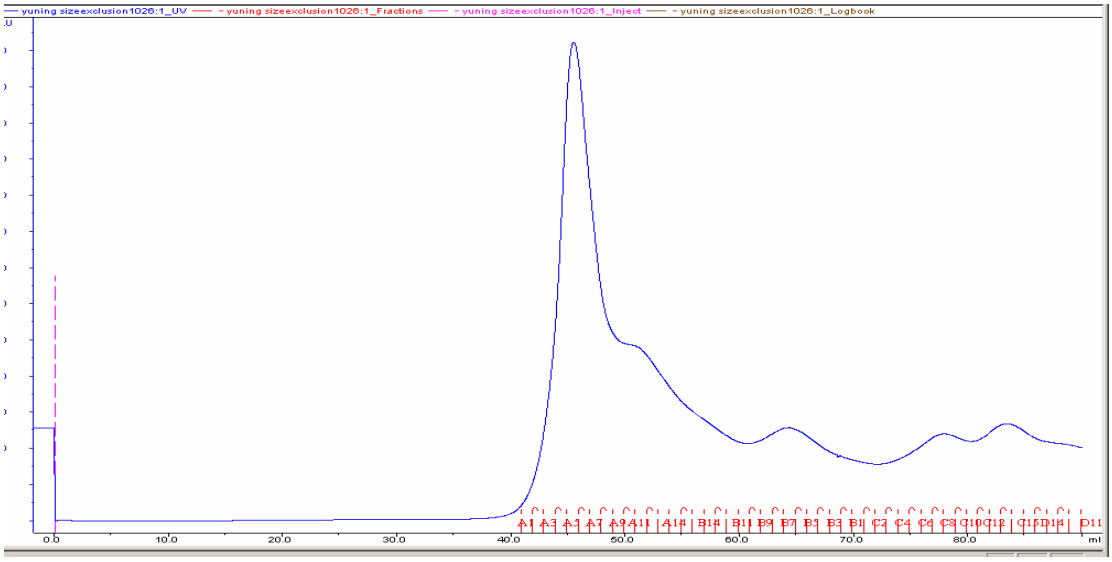

Figure 4.3.1 FPLC UV spectrum of the random coil domain of EEN. The main peak is from fractions with elution volumes for protein bigger than 80 kDa, which was supposed to be self-aggregated proteins.

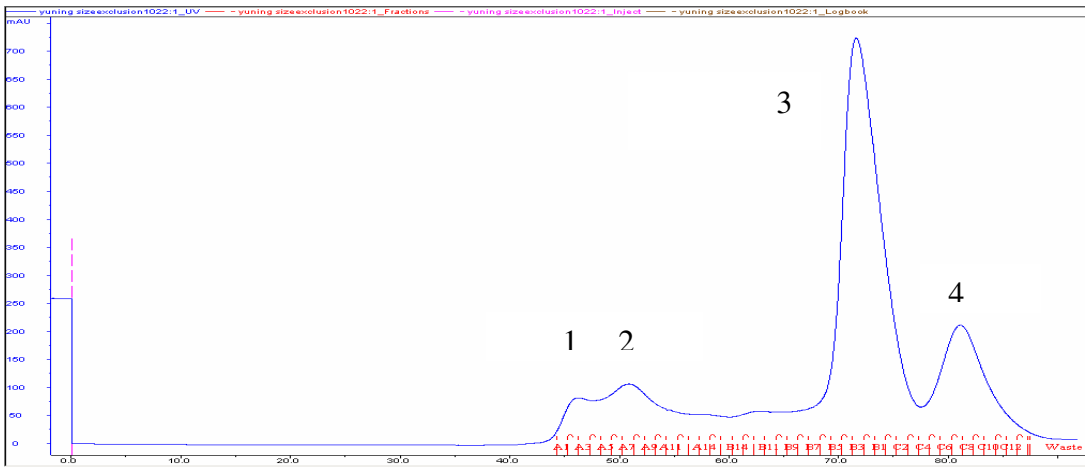

Figure 4.3.2 FPLC UV spectrum of ΔBAR domain of EEN during purification.

A:

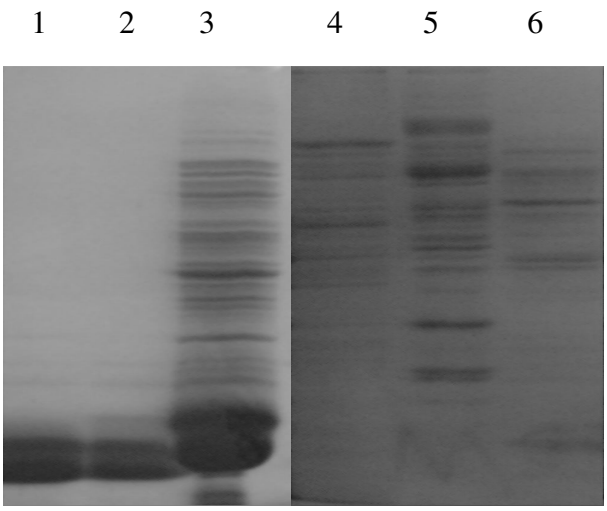

Figure 4.3.3 A: SDS PAGE of EEN ΔBAR expressed in BL21 DE3. Lane 1 and 2: the sample from peak 3 in FPLC; Lane 3: the samples after Ni-NTA affinity column. Lane 4: the sample form peak 1 in FPLC; Lane 5: the sample form peak 2 in FPLC; Lane 6: the sample from peak 4 in FPLC.

B:

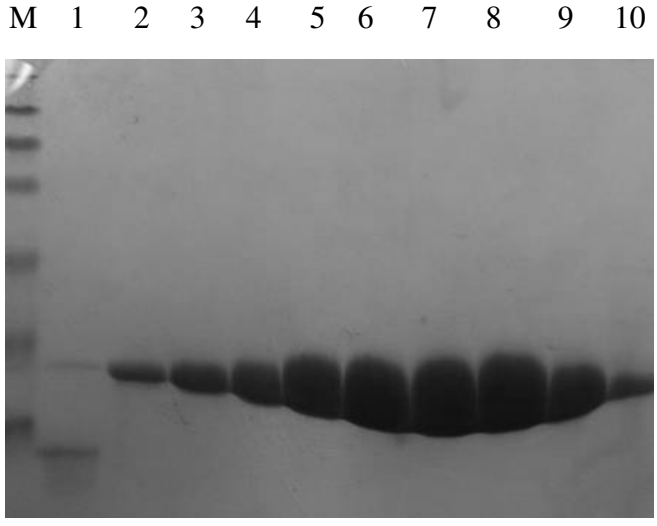

Figure 4.3.3 B: SDS PAGE study on EEN ΔBAR expressed in M9. Lane 1 to 10: the 10 samples from the highest peak in FPLC.

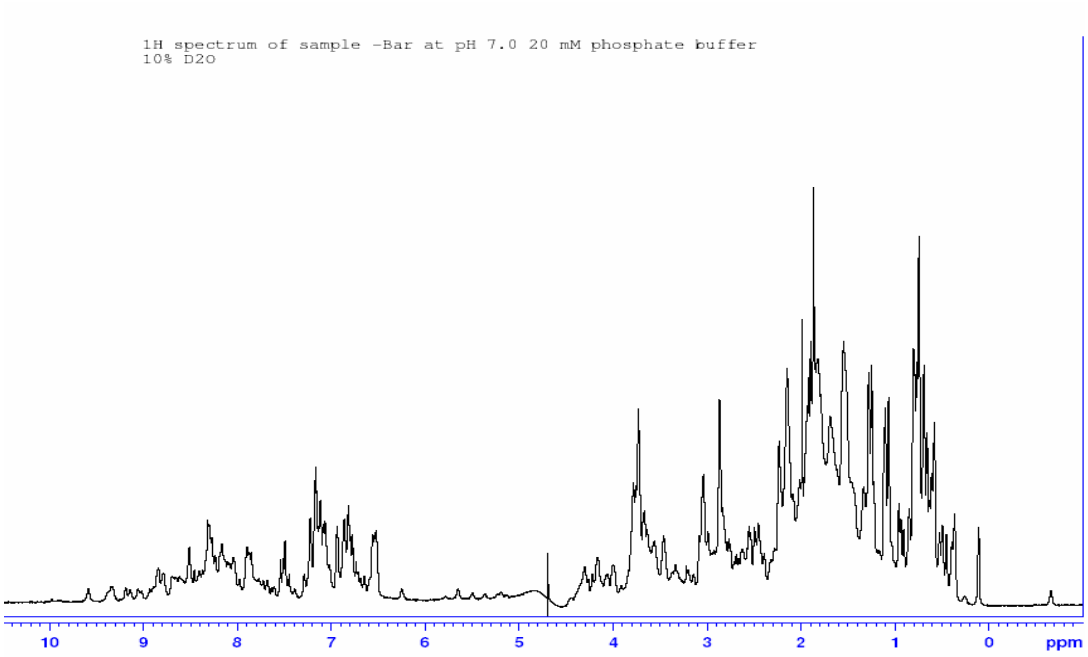

Figure 4.3.4 1-D NMR Study on ΔBAR domain of EEN.

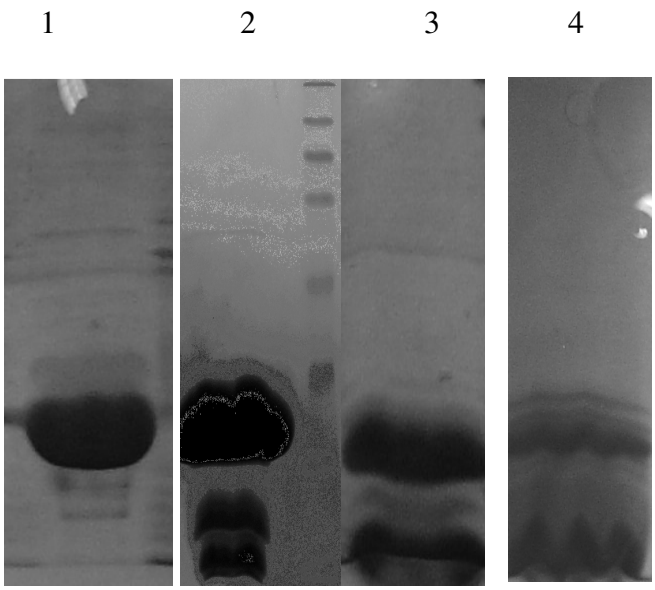

Figure 4.3.5 SDS PAGE study on the degradation of ΔBAR domain of EEN. Lane 1: the purified ΔBAR at the first day; Lane 2: the purified ΔBAR after 3 days at the room temperature; lane 3: the purified ΔBAR after 7days at the room temperature; lane 4: the purified ΔBAR after 2 weeks.

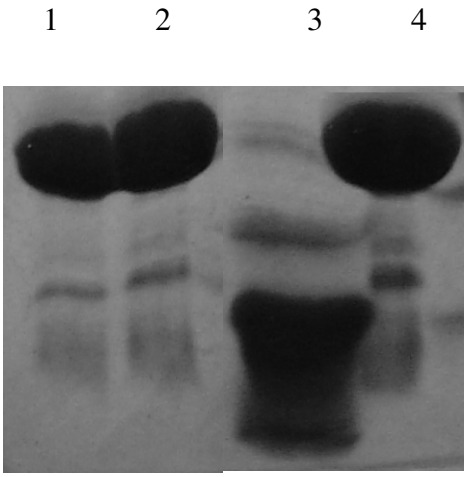

Figure 4.3.6 SDS PAGE study on the degradation of ΔBAR domain of EEN. Lane 1: fresh purified ΔBAR domain in 1XPBS, 1mMDTT; Lane 2: fresh purified ΔBAR domain in phosphate buffer without salt, pH 7.4; Lane 3: ΔBAR domain in phosphate buffer after 3 days; lane 4: ΔBAR domain in 1XPBS after 3 days.

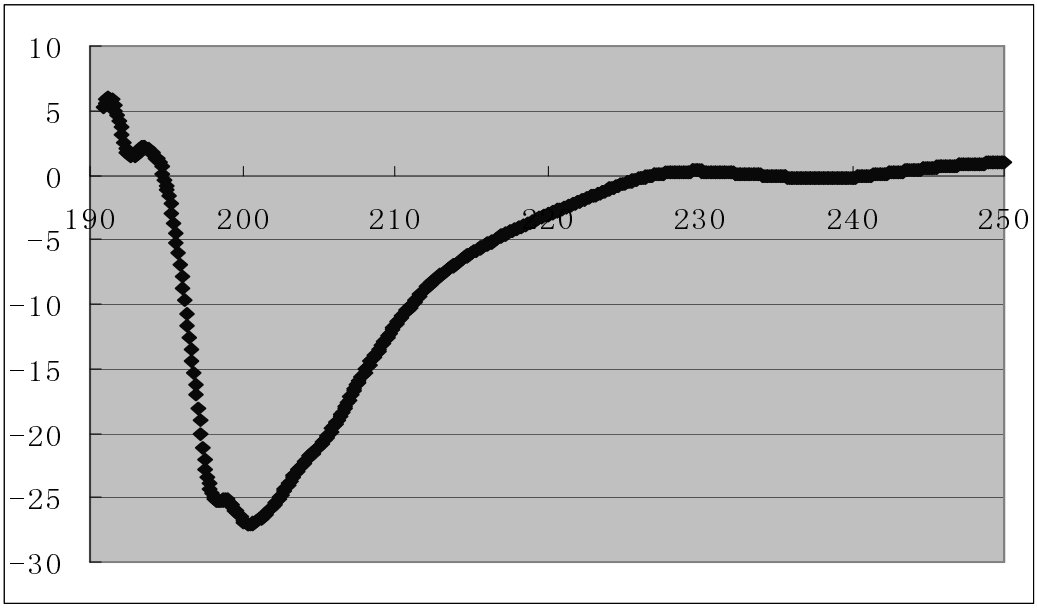

Figure 4.3.7 CD spectrum of EEN ΔBAR scanning from 190nm to 250nm.

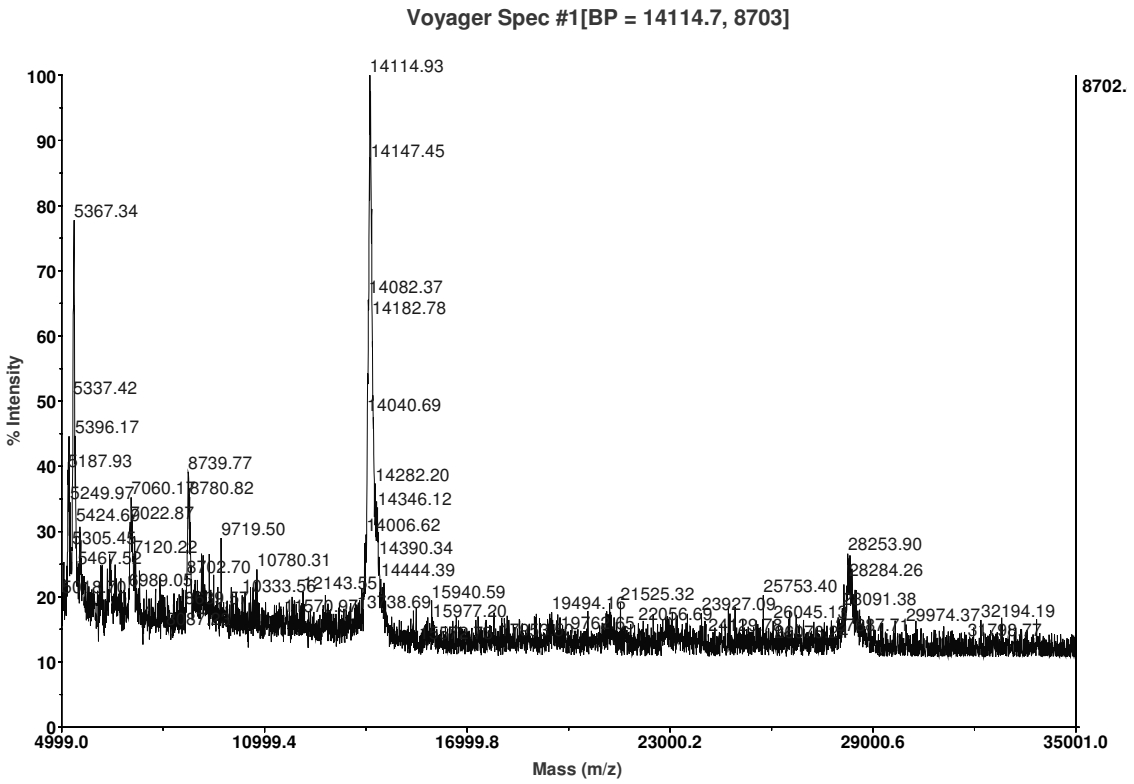

Figure 4.3.8 Multi-TOF MS spectrum of EEN Δ Bar domain.

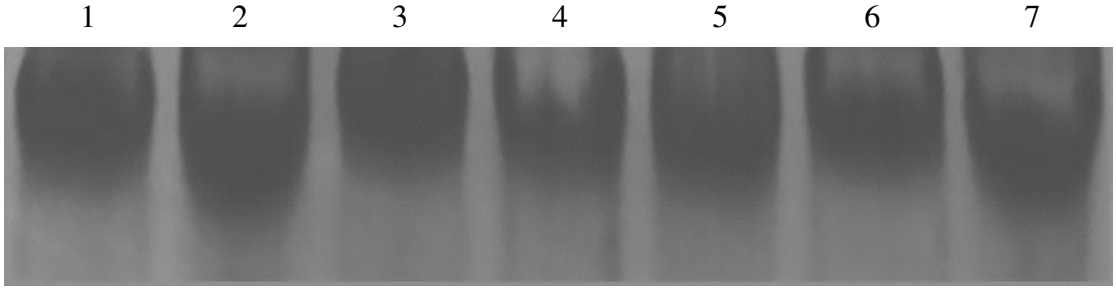

Figure 4.3.9 Native PAGE of EEN Δ BAR. Lane1: control ; lane 2: 5μM EGTA, lane 3: 5μM Ca^{2+}; lane 4: 10μM Ca^{2+}; lane 5: 15 μM Ca^{2+}; lane 6: 20 μM Ca^{2+} ; lane 7: 25μM Ca^{2+}.

The CD spectrum suggested a notable feature of ß−sheet in Δ BAR domain (Figure 4.3.7). The stability of the peptide was dependant on the amount of salt in the buffer. When the concentration of the salt was below 100mM, the percentage of the degradation was more than 90% after 3 days (Figure 4.3.5 and 4.3.6). In contrast, when the concentration of the salt was 150mM, the percentage of the degradation was less than 10% after 7 days at 4 degree even when concentration of the peptide was as high as 2-3 mM (Figure 4.3.5 and 4.3.6).

To identify the main degradation product of EEN Δ BAR, the purified Δ BAR domain was subjected to the Multi-TOF MS after storage at room temperature for five days (Figure 4.3.8). The result suggested that the main degradation product was a small peptide of size around 5.3 kDa. However, identity of the peptide was not determined.

The proline rich domain that exists at the random coil region showed a very weak binding to SH3 domain (Table 4.3.1). It was hypothesized that the EEN SH3 domain binding to its proline rich domain at a Ca^{2+} dependant manner (Yuan et al., 2004).

The native PAGE results showed that no change was observed when the concentration of Ca^{2+} was increased (Figure 4.3.9). Meanwhile, NMR

titration of the Ca^{2+} to the Δ Bar was performed. The result also suggested that Ca^{2+} does not interact or affect the conformation of ΔBAR even at a very high concentration of Ca^{2+} (data not shown here).

The result may due to the lack of post-translate modification to the EEN by the BL21(DE3) expression system. The Ca^{2+} channel may also be required before the proper interaction can be observed between Ca^{2+} and the random coil region.

4.4 expression and purification of SH3 domain

SH3 domain of EEN was designed based on the secondary structure prediction and BLAST sequence comparison with the SH3 domain family (Table 4.3.1). It is a highly conserved domain among the SH3 domain containing proteins family.

The SH3 domain of EEN was over-expressed in the BL21 system as soluble monomeric protein without self-aggregation products as observed during the purification with affinity column and FPLC (Figure 4.4.1). The stability of the protein was also partially dependant on the amount of salt in the buffer, but is considerably higher than that of ΔBAR domain under the same buffer condition.

However when the His-tag was cleaved away from the SH3 domain using thrombin at 37ºC, non-specific cleavage on the protein was observed. Even though the reaction was performed at lower temperature (4 ºC) and lower concentration of thrombin, no specific cleavage can be observed (Figure 4.4.2 and 4.4.3).

Due to difficulty in removing the tag from the SH3 domain, a new express system was used. The Nde1 cutting site was chosen instead of the BamH1 cutting site. As a result, the His Tag would not be expressed in this system. The expression level was similar to the one with His tag. The use of ion-exchanger for purification of the un-tagged protein did not improve purity of the protein.

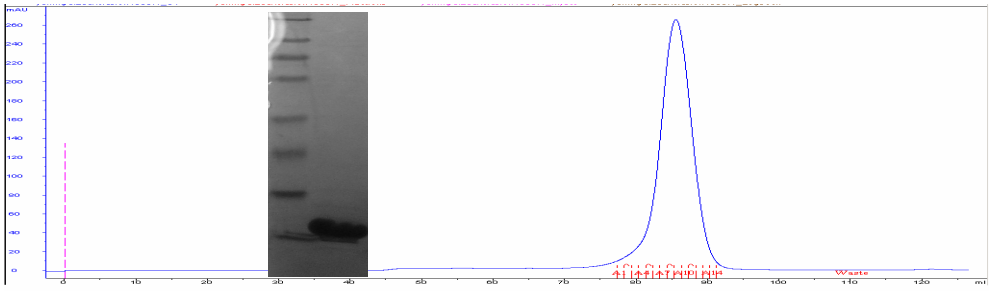

Figure 4.4.1 FPLC UV Spectrum of SH3 domain of EEN. The left picture inserted is the SDS PAGE of the purified SH3 domain after FPLC

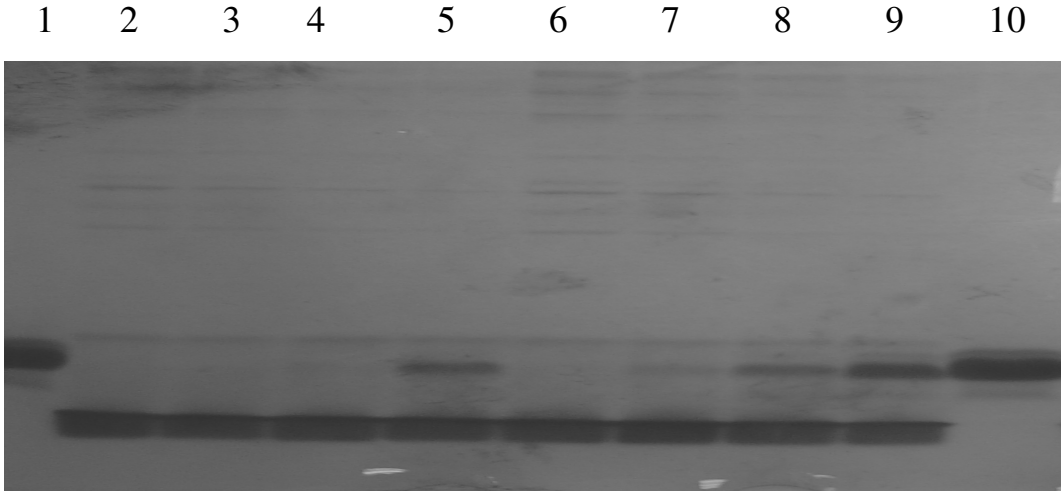

Figure 4.4.2 SDS PAGE study on the thrombin cleavage effect on SH3 domain. Lane 2 to 4: using 50 unit thrombin for 0.5 hour, 1 hour, 2 hours separately before running FPLC; Lane 5 to 7: using 30 unit thrombin for 0.5 hour, 1 hour, 2 hours separately before running FPLC; Lane 8 and 9: using 20 unit and 10 unit thrombin separately for 0.5 hour before running FPLC; Lane 1 and 10: negative controls. All the cleavages were performed under room temperature. The volume of the SH3 domain studied is about 2 μM.

M 1 2 3 4 5 6 7 8 9 10 11 12 13

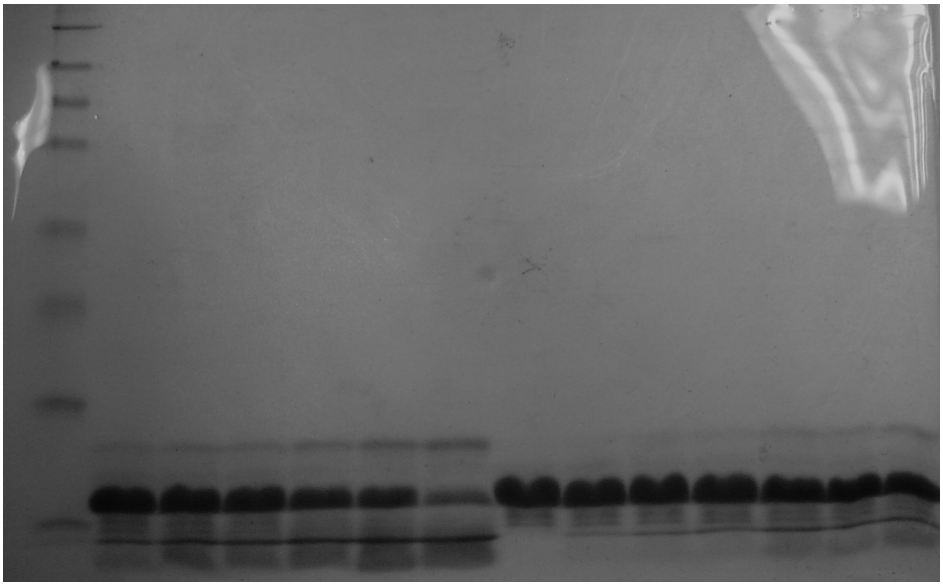

Figure 4.4.3 SDS PAGE study on the thrombin cleavage effect on SH3 domain. Lane 1 to 6: using 50 unit thrombin for 1 hour, 2hours, 3 hours,4 hours, 5 hours, and 6 hours separately at 4°c; Lane 7: the control without cleavage; Lane 8 to 13: using 10 unit thrombin for 1 hour, 2hours, 3 hours,4 hours, 5 hours, and 6 hours separately at 4°c.

The volume of SH3 domain studied was about 2 μM.

4.5 Expression and Ca^{2+} binding ability study of SH3p11

Due to failure in detecting the Ca^{2+} binding activity in EEN, the rat homologue of EEN called SH3p11was was also cloned and tested for Ca^{2+} binding ability. SH3p11 was shown to bind Ca^{2+} channel in vivo and the interaction was confirmed to be Ca^{2+} dependent (Chen et al., 2003).

Using cDNA from rat liver as the template, the 2-steps PCR was performed to obtain the gene coding for SH3p11. The cloned SH3p11 was then expressed in BL21 (DE3) with the same procedure as EEN. The domain in SH3p11 corresponding to the ΔBAR domain of EEN was cloned and expressed as well. Both SH3p11 full length and ΔBAR domain of SH3p11 did not show binding of Ca^{2+} as confirmed by native PAGE and 2D NMR titration experiments respectively.

4.6 Cloning and expression of proline rich domain peptide

The PRD of BPGAP1 shows the highest affinity to the endophilin SH3 domain among the PRD containing proteins family. The sequence of this peptide derived from the PRD of BPGAP1 contains the sequence motif of "PPPXPP" (Table 4.6.1)

T K T P P P R P P L P T Q

Table 4.6.1 Amino Acids Sequence of the Proline rich domain of BPGAP1.The underline amino acids is the motif responsible to the binding of the SH3 domain of endophilin.

The proline rich domain peptide of BPGAP1 was cloned and expressed to investigate its binding activity to the ΔBAR and SH3 domain of EEN. The expression level of GST-fusion peptide in BL21 system was quite high (induced at 37ºC for 5 hours), and consistent level of expression was observed at different temperature and IPTG concentration for induction (Figure 4.6.1).

The sample of proline rich domain peptide was subjected to Multi-TOF MS after purification by the Ni-NTA affinity column and HPLC. The Multi-TOF MS result suggested a sample of very high purity (Figure 4.6.2).

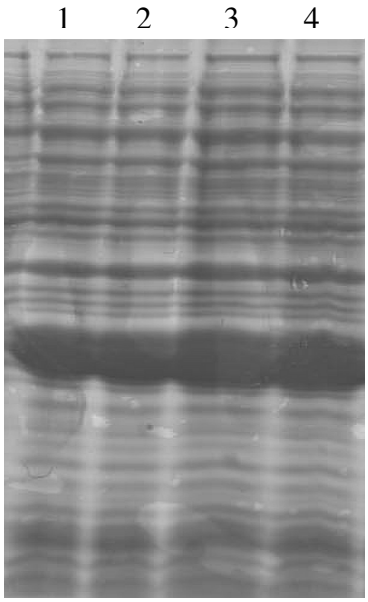

Figure 4.6.1 SDS PAGE of the PRD expression in BL21. Lane1: inducing with 0.1mM IPTG at 37ºc for 5 hours; Lane 2: inducing with 05mM IPTG at 37ºC for 8hours; Lane 3: inducing with 0.1mM IPTG at 20°C for 12 hours; lane 4: inducing wit 0.5mM IPTG at 20°C for 12 hours.

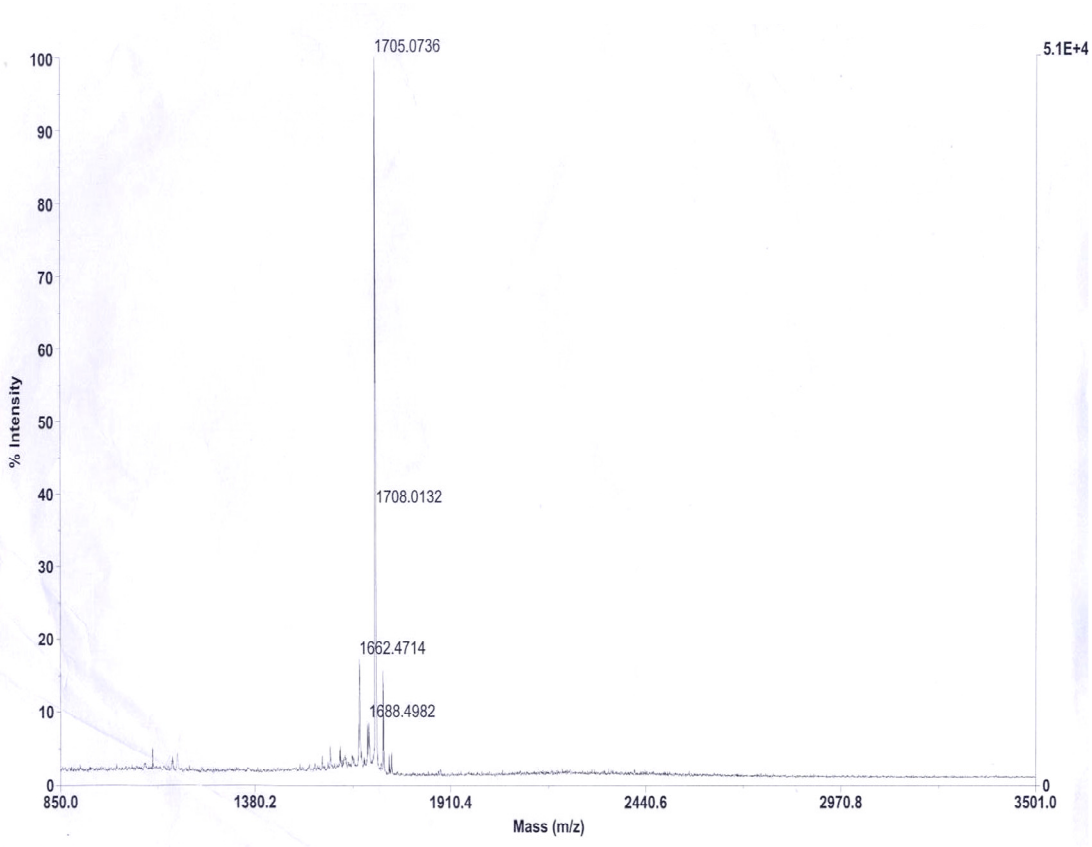

Figure 4.6.2 Multi-TOF MS Spectrum of purified Proline rich domain. The theory molecular weight of PRD is 1705 Da.

4.7 ITC study on the binding affinity of PRD to the ΔBAR domain and SH3 domain of EEN

Isothermal Titration Calorimetry (ITC) monitors and quantifies binding affinity through measurement of the tiny amounts of heat release that released during titration of Proline rich domain (PRD) peptide in to EEN.

Form the result of the ITC, the binding affinity of SH3 domain to the proline rich domain was determined to be 9.8 μM, while the binding affinity of the ΔBAR domain to the proline rich domain was 13.3 μM. The results indicate that the PRD of BPGAP1 bind to the ΔBAR and SH3 domain of EEN at similar affinities (Figure 4.7.1 and 4.7.2).

Both titrations were performed under similar conditions with identical protein concentrations and buffers. The concentrations of the proteins were calculated based on their UV absorption value (Table 4.7.1 and 4.7.2). In conclusion, the random coil PRD of EEN at the N-terminal region of ΔBAR has no effect on the interaction between SH3 domain and PRD peptide from BPGAP1.

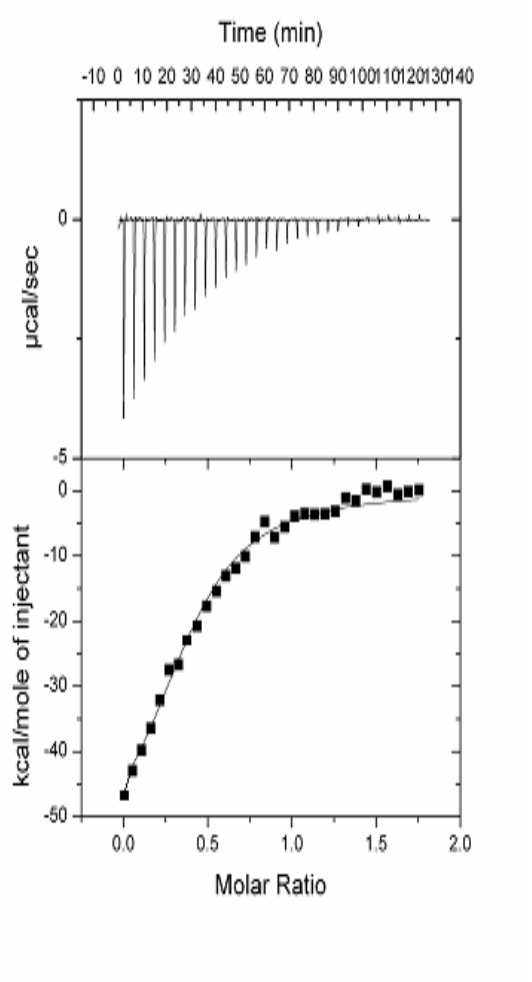

Kd = 9.837 ± 0.9524 uM

R Δ 2 = 0.9793

Figure 4.7.1 ITC binding fitting study on SH3 domain to Proline rich domain.

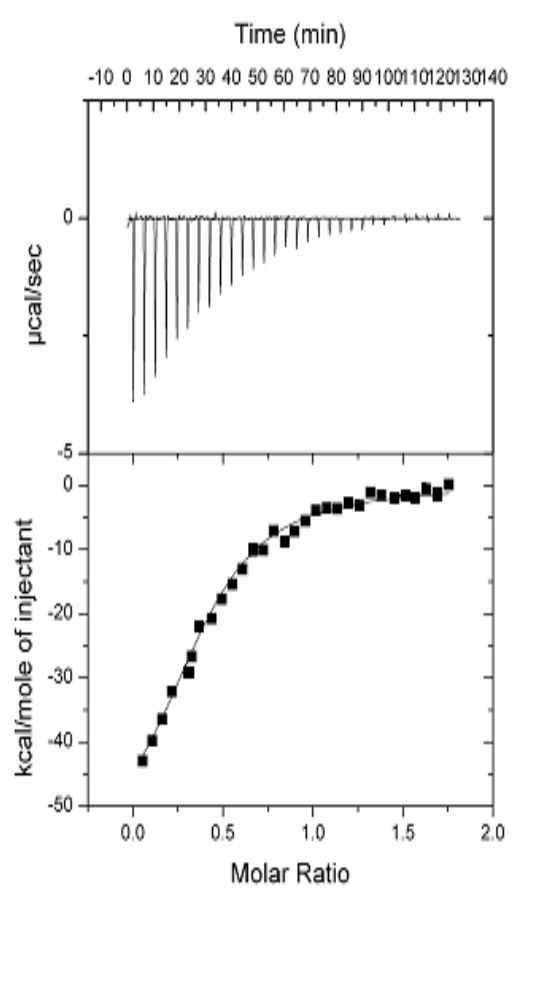

Kd = 13.321± 0.9926 u M

R Δ 2 = 0.9892

Figure 4.7.2 ITC binding fitting study on Δ BAR domain to Proline rich domain.

	276 nm	278 nm	279 nm	280 nm	282 nm
Ext. coefficient	9750	9800	9695	9530	9200
Abs 0.1% (=1 g/l)	1.330	1.336	1.322	1.300	1.255

	276 nm	278 nm	279 nm	280 nm	282 nm
Ext. coefficient	9750	9800	9695	9530	9200
Abs 0.1% (=1 g/l)	1.330	1.336	1.322	1.300	1.255

Table 4.7.1 SH3 domain Extinction coefficients prediction using ProtParam web tool in units of M^{-1} cm^{-1}. The first list values computed assuming all Cys residues appear as half cystines, whereas the second list values assume that none do.

	276 nm	278 nm	279 nm	280 nm	282 nm
Ext. coefficient	11345	11327	11160	10930	10520
Abs 0.1% (=1 g/l)	0.811	0.810	0.798	0.782	0.752

	276 nm	278 nm	279 nm	280 nm	282 nm
Ext. coefficient	11200	11200	11040	10810	10400
Abs 0.1% (=1 g/l)	0.801	0.801	0.790	0.773	0.744

Table 4.7.2 Δ BAR domain Extinction coefficients prediction using ProtParam web tool in units of M^{-1} cm^{-1}. The first list values computed assuming all Cys residues appear as half cystines, whereas the second list values assume that none do.

4.8 NMR study on Δ BAR domain and SH3 domain of EEN

4.8.1 Assignment of SH3 domain and Δ Bar domain

N-15 labelled SH3 domain and Δ BAR domain of EEN expressed in M9 with 20% glucose (1g/L $^{15}NH_4Cl$) was used for sequential assignment. TOCSY and NOESY spectra of SH3 and Δ BAR domains were obtained on a 800 MHz NMR performed at 298K. Using the software SPARKY, all the 59 amino acids of the SH3 domain were assigned except for the 7 prolines that did not show up on HSQC. For the Δ BAR domain, 82 amino acids including the 59 amino acids from the SH3 domain were assigned based on the 3D NMR experiments (Table 4.8.1.1 and 4.8.1.2; Figure 4.8.1.1 and 4.8.1.2). Still there were some residues that were not assigned in the Δ BAR domain due to the resonance overlap and weak peaks. These residues did not seem to be involved in binding of the praline rich domain.

1	MPPLDQPSCKA LYDFEPENDG ELGFHEGDVI TLTNQIDENW YEGMLDGQSG FFPLSYVEV 60
61	LVPLPQ

Table 4.8.1.1 SH3 domain sequence in NMR HSQC. All the residues except for the Prolines were assigned in the HSQC spectrum.

-58	MREASSRPKR EYKPKPREPF DLGEPEQSNG GFPCTTAPKI AASSSFRSSD KPIRTPSRS 0
1	MPPLDQPSCKA LYDFEPENDG ELGFHEGDVI TLTNQIDENW YEGMLDGQSG FFPLSYVEV 60
61	LVPLPQ

Table 4.8.1.2 Δ BAR domain sequence in NMR HSQC. Underline residues were already assigned in HSQC spectrum except for Prolines.

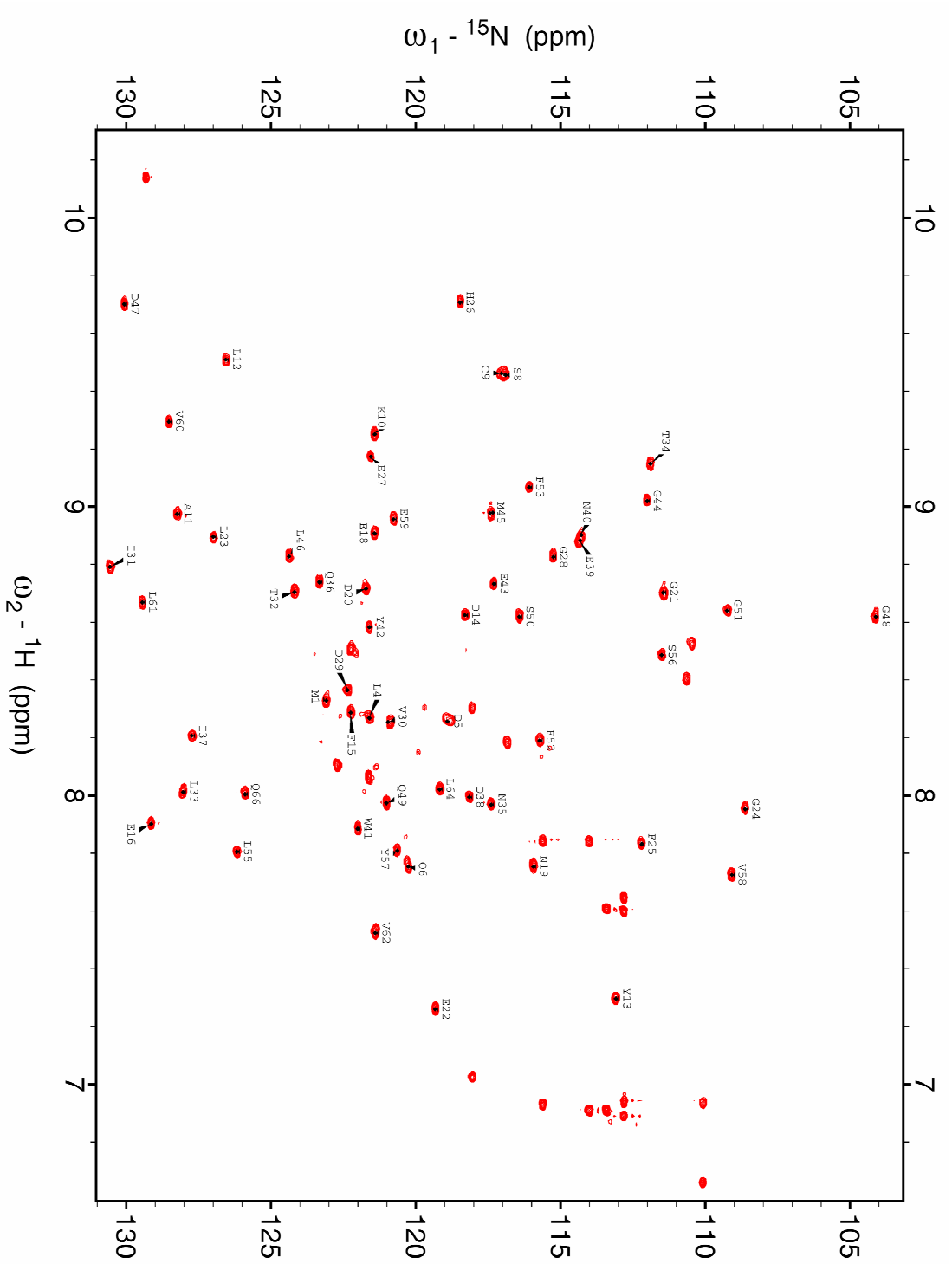

Figure 4.8.1.1 The HSQC spectrum of SH3 domain of EEN.

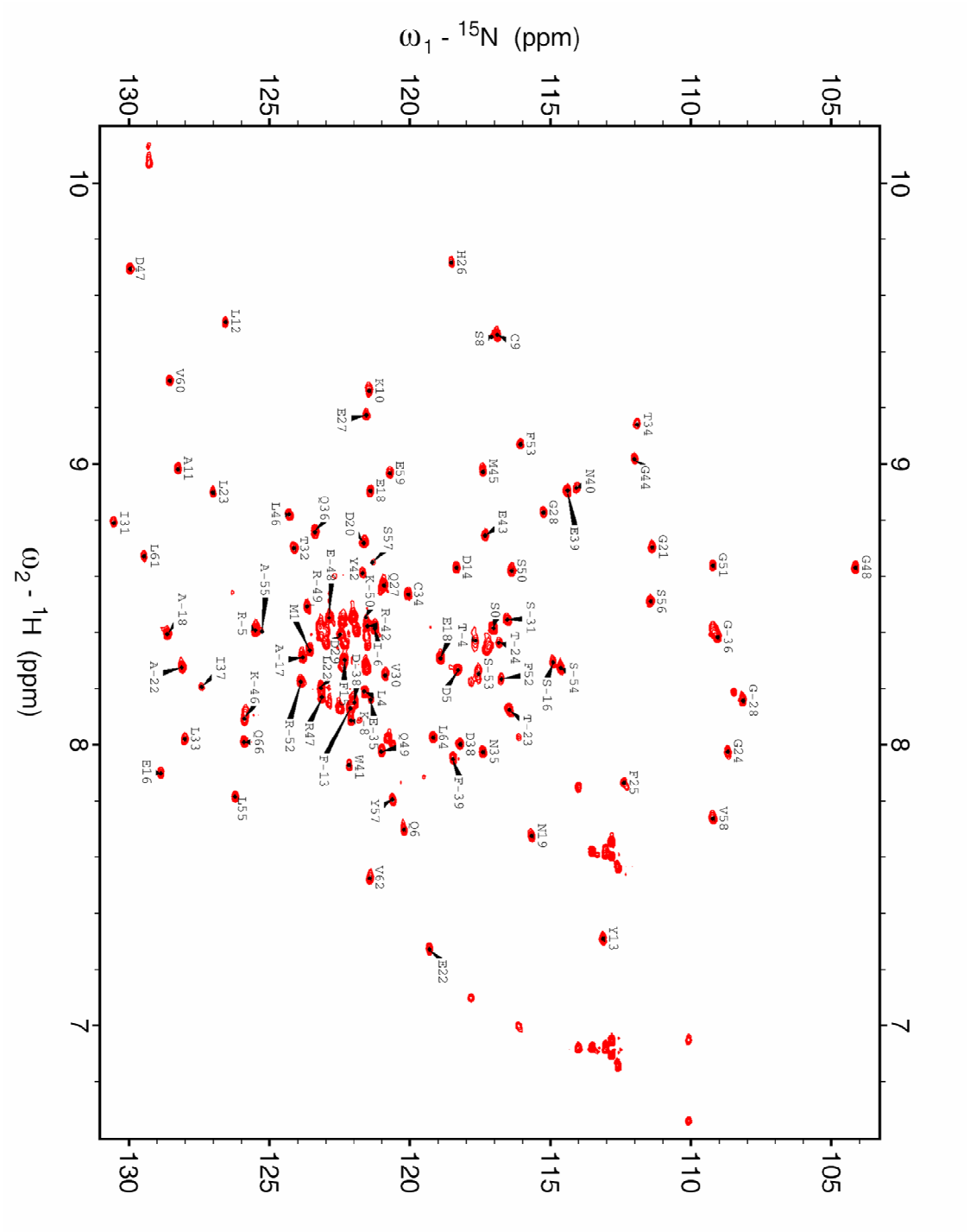

Figure 4.8.1.2 The HSQC spectrum of ΔBAR domain of EEN.

4.8.2 NMR study on the binding affinity of SH3 domain and ΔBAR domain to proline rich domain

The concentration of the SH3 domain used was 85.5 μM while that of the proline rich domain peptide was 4.6 mM. A 2-D HSQC NMR spectrum was recorded every time after addition 3 μl of proline rich domain peptide into the SH3 sample (25mM PIPES, 150mM NACL,4mM DTT pH 6.5) until further chemical shift perturbation was not observed on the HSQC spectrum. The reference HSQC spectrum of SH3 clone was overlaid with the spectrum of SH3 saturated with praline rich domain for comparison (Figure 4.8.2.2).

Seven residues (G24, F25, I37, L55, S56, Y57, V58) which had the highest extent of chemical shift perturbation were used to determine the binding affinity using the following equation on the software Origin 7.0 (Table 4.8.2.1; Figure 4.8.2.1).

$$Y=F0 + (Ff-F0)* \{ X+[Prot]+Kd -\sqrt{((X + [Prot]+Kd)^2 - 4[L][Prot])} \} / 2[Prot]$$

Table 4.8.2.1 The fitting function of binding affinity. Y stands for the chemical shift of the point. X stands for the ligand concentration. [Prot] stands for the protein concentration. Ff stands for the final chemical shift of the point. F0 stands for the initial chemical shift of the point.

For the Δ Bar domain, the protein concentration was 83 μM while the concentration of the proline rich domain peptide was 4.6 mM. The 2-D NMR titration was performed by addition 3 μL of proline rich domain peptide into the protein sample (25mM PIPES, 150mM NACL, 4mM DTT pH 6.5), until saturations was observed. After titration, the reference Δ BAR domain's HSQC spectrum was compared with the one of ΔBAR domain saturated with the proline rich domain (Figure 4.8.2.3).

Seven residues (G24, F25, I37, L55, S56, Y57, V58) which showed the biggest changes on chemical shift were used to determine the binding affinity (Figure 4.8.2.4).

For both the ΔBAR and SH3 domain, the residues that were perturbed upon titration with PRD are similar and mostly from the SH3 domain but not from the random coil region of the ΔBAR domain.

Among the seven residues perturbed, 3 residues (L55, S56, Y57 in SH3 domain and ΔBAR domain) were responsible for the direct binding of the proline rich domain according to the secondary structure prediction (Figure4.8.2.5).

The fitting result suggested that the binding affinity of the SH3 domain to the Proline rich domain was about 1.24 μM, while the binding affinity of the ΔBAR domain to the Proline rich domain was about 2.68 μM.

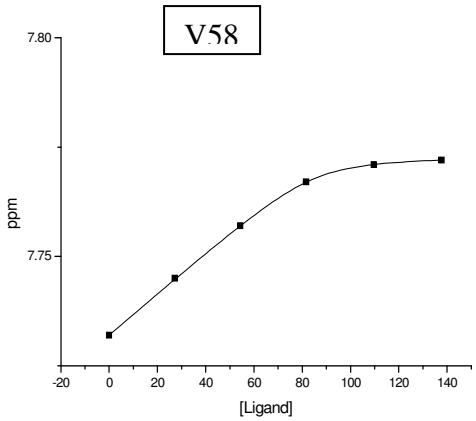

Kd 1.63±0.178 μM; R^2 0.9995

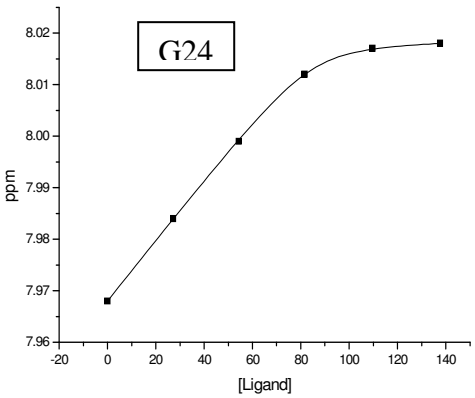

Kd 1.34± 0.177μM; R^2 0.9994

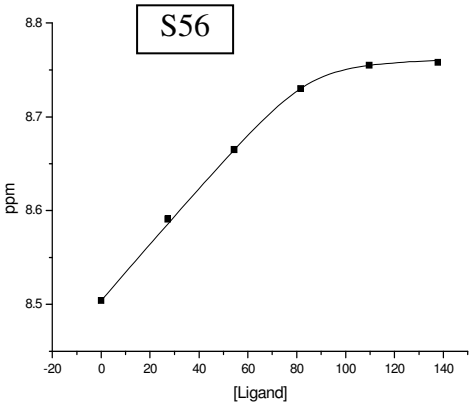

Kd 1.23±0.538 μM; R^2 0.99936

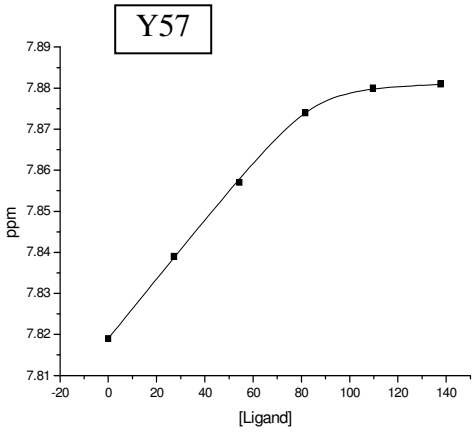

Kd 1.07±0.338 μM; R^2 0.9997

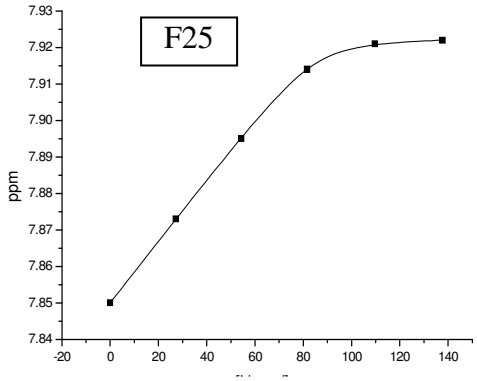

Kd 1.02±0.113 μM; R^2 0.99996

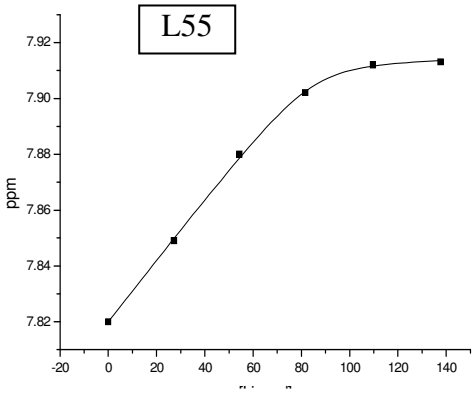

Kd 1.26± 0.46μM; R^2 0.99955

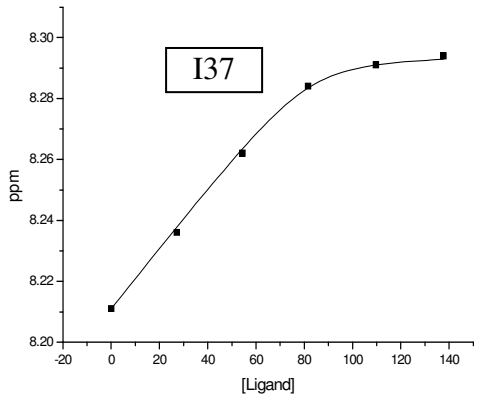

Kd 1.16±0.466 μM; R^2 0.9995

Figure 4.8.2.1 The seven residues (G24, F25, I37, L55, S56, Y57, V58) binding affinity fitting curve of SH3 domain to PRD by the Origin 7.0. The average Kd value was about 1.24 μM.

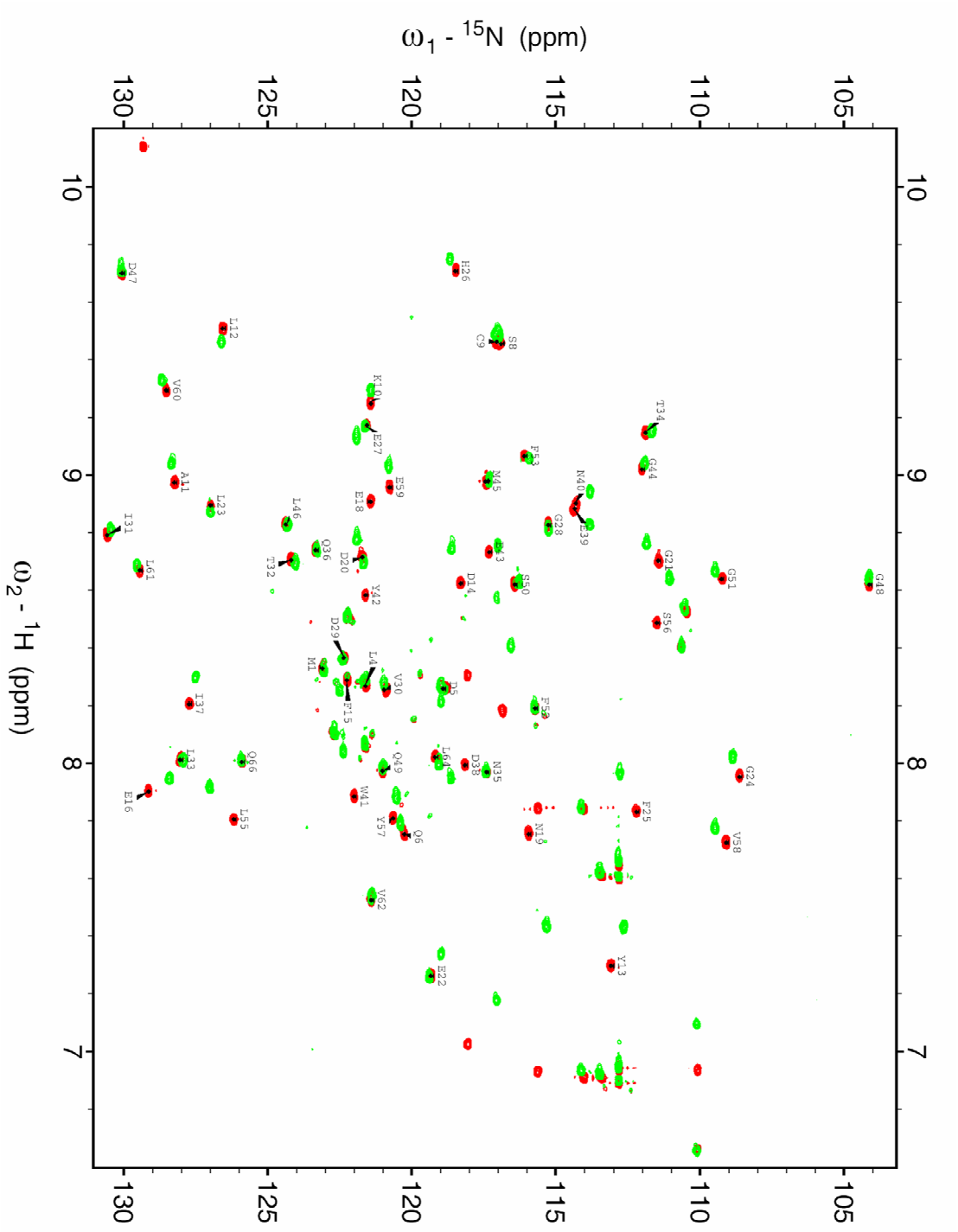

Figure 4.8.2.2 NMR HSQC spectrum of SH3 domain. Those depicted in red stand for the initial chemical shifts of SH3 domain without titration, those depicted in green stand for the final chemical shifts of SH3 domain in the titration.

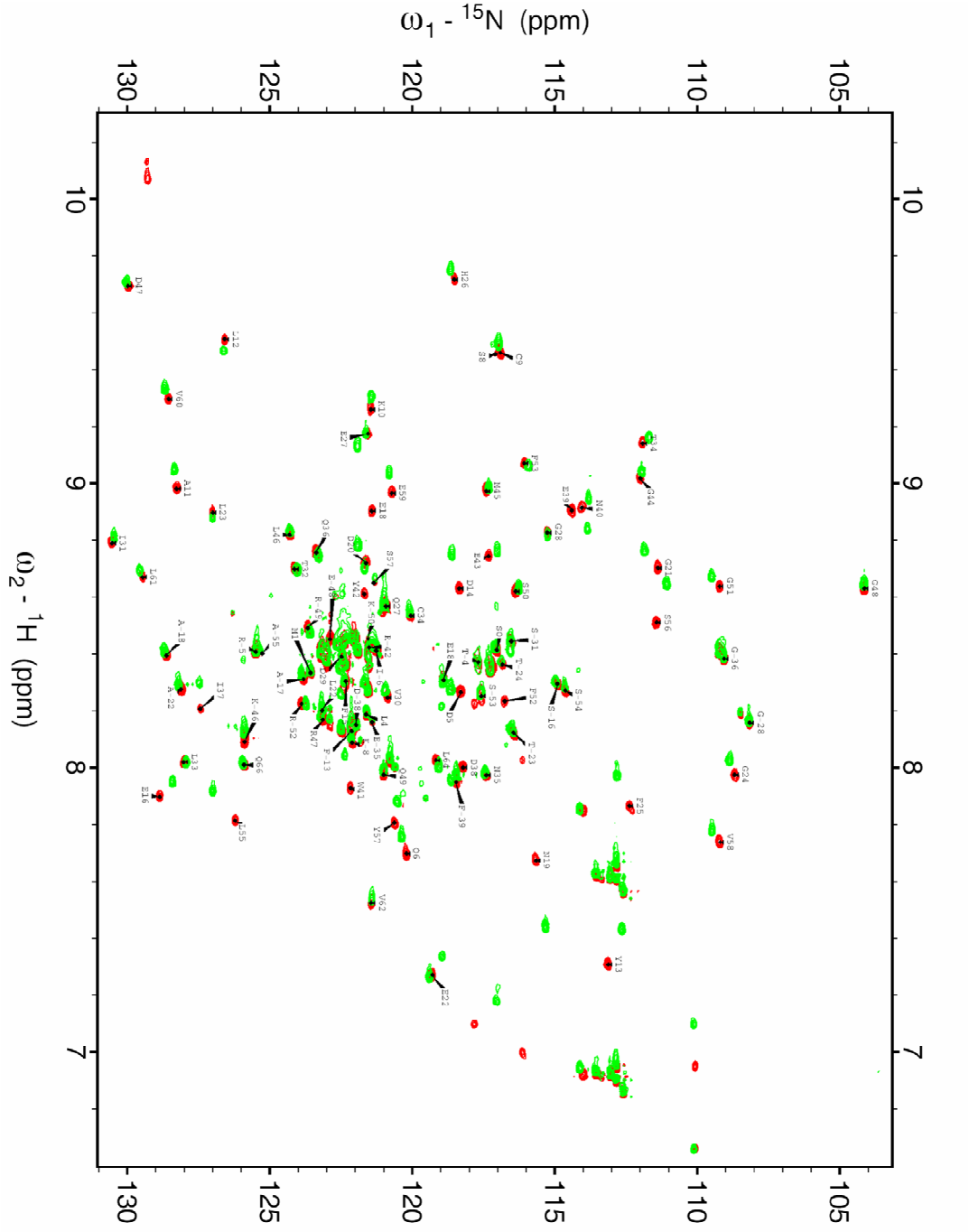

Figure 4.8.2.3 ΔBAR domain HSQC spectrum. Those depicted in red stand for the initial spectrum without titration, those depicted in green stand for the final spectrum of the titration.

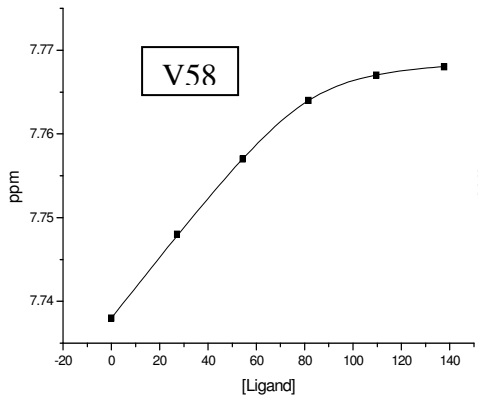

Kd 2.73±0.248 µM ; R^2 0.99996

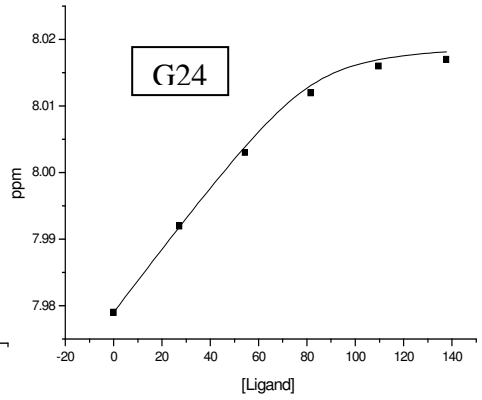

Kd 2.37± 0.266 µM ; R^2 0.99994

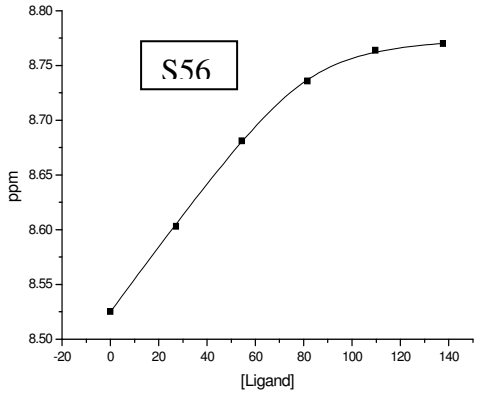

Kd 2.76±0.566 µM ; R^2 0.99978

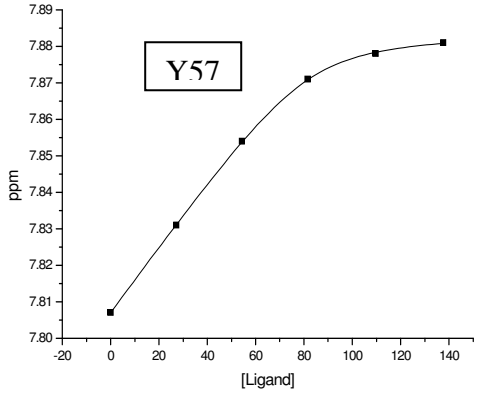

Kd 2.71±0.295 µM; R^2 0.99994

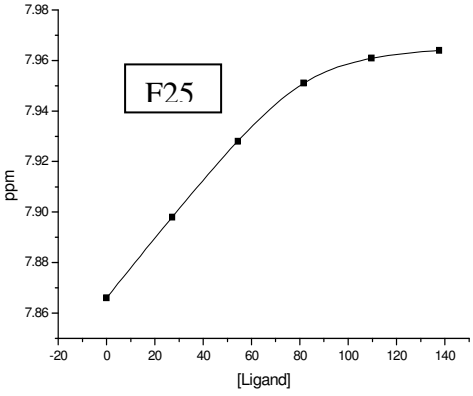

Kd 2.58± 0.092µM ; R^2 0.99999

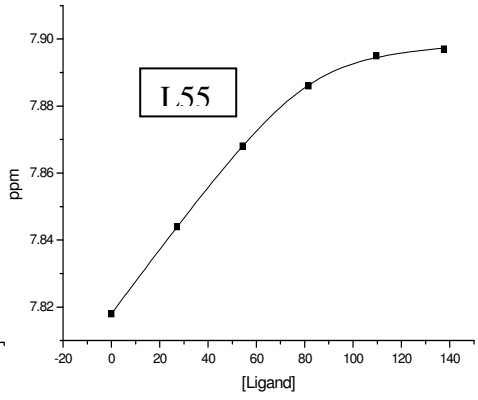

Kd 2.99±0.378µM ; R^2 0.99991

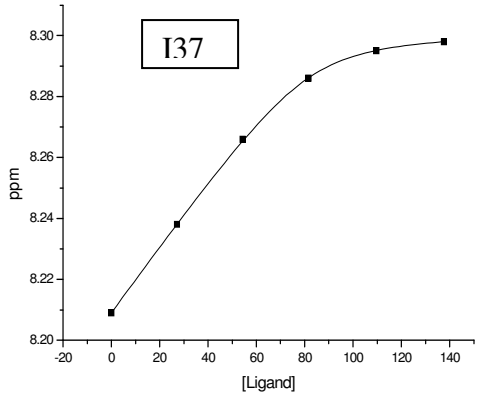

Kd 2.65±0.248 μM ; R^2 0.99994

Figure 4.8.2.4 The seven residues (G24, F25, I37, L55, S56, Y57, V58) binding affinity fitting curve of SH3 domain to PRD by the Origin 7.0. The average Kd value was about 2.68 μM.

Figure 4.8.2.5 Secondary structure prediction of SH3 domain of EEN. The deep pink colour part stands for the directly PRD binding domain residues including L55, S56 Y57.

CHAPTER 5 DICUSSION

5.1 The *in vitro* Ca^{2+} binding ability of Endophilin A2 family

Based on the NMR study on the full length EEN as well as its three domains (BAR domain, SH3 domain and ΔBAR domain), Ca^{2+} does not seem to perturb chemical shifts of any residues of EEN *in vitro* during titration. The secondary structure of the EEN also remains unchanged in the presence and absence of Ca^{2+} *in vitro* based on CD and NMR studies. Native PAGE study also suggests that EEN does not interact with Ca^{2+} *in vitro*. The same result was obtained when the rat homologue of EEN, SH3p11 was used for the experiments.

The binding of $Ca^{2+,}$ however, was shown to be essential for the formation of the complex of endophlin A2 and the Ca^{2+} channel *in vivo*. This interaction requires only a relatively low concentration of Ca^{2+} at around 300 nM (Chen et al., 2003). There are two possible explanations for the failure of detection of Ca^{2+} binding on EEN. Firstly, the presence of the Ca^{2+} channel *in vivo* might be required for the interaction between Ca^{2+} and EEN. Secondly, EEN expressed in prokaryotic system does not have the necessary post-translated modification for it to function properly.

5.2 The binding affinity of EEN SH3 domain and EEN ΔBAR domain to PRD

Both of the NMR and ITC studies suggested that the PRD of BPGAP1 binds similar to the SH3 domain and ΔBAR domain. Based on the 2-D NMR study, residues in the random coil domain are not involved in binding the PRD. Compared with the other SH3 domain containing proteins, the binding affinity of EEN to PRD was higher, which is not comparable with the binding affinity of antibody to antigen that was around nano-molar to pico-molar level (Table 5.2.1).

EEN uses its SH3 domain to bind many PRD containing proteins in clathrin mediated synaptic endocytosis, such as BPGAP, amphyphisin, etc. while the BAR domain bind or bend the cell membrane *in vivo*. The random coil region between BAR domain and SH3 domain acts as a bridge to connect these two domains.

However, the results in this project suggested that the random coil region is not involved in the interaction of SH3 domain and BPGAP1. It is also unlikely that this random coil region will assist the BAR domain in binding or bending to the cell membrane based on previous studies on BAR domain containing proteins.

	Bind affinity(Kd)
Sem5 SH3 domain	54 μM
Mouse Crk SH3 domain	6 μM
Mouse Src SH3 domain	25 μM
Human Grb2 SH3 domain	5 μM
Human EEN SH3 domain	1.5 μM

Table 5.2.1 The binding affinity of SH3 domain containing proteins to PRD.

CHAPTER 6

CONCLUSIONS AND FUTURE PERSPECTIVES

6.1 Conclusions

The *in vitro* properties of the random coil domain connecting the BAR and SH3 domain of EEN were studied in this work. Using the BL21 DE3 system, the full length EEN and its three domains (BAR domain, SH3 domain, Δ BAR domain) were expressed.

After purification with affinity column and FPLC, the full length EEN's dimer was very unstable *in vitro* and tend to aggregate quickly especially at high concentration. Based on CD and NMR studies, both the BAR domain and full length EEN does not interact with Ca^{2+} at up to 10 μM.

In contrast, Δ BAR and SH3 domain are much more stable. The process of degradation was slow even at high protein concentration. Using 3D-NMR, the resonances of SH3 domain and Δ BAR domain were assigned. No obvious chemical shift perturbation was observed in the presence of increasing concentration of (0~10μM) Ca^{2+}.

The effect of the random coil region on the binding ability of the EEN SH3 domain to the PRD of BPGAP1 was also investigated. ITC and NMR titration were used to quantitatively monitor the changes in both SH3 and Δ BAR domains upon binding to the PRD. The binding affinities of these two domains were similar based on titration results from HSQC NMR spectra.

6.2 Future Perspectives

As EEN is a eukaryotic protein, those eukaryotic express systems such as 293T Epithelium or NIH3T3 Fiberoblast should be considered to for expression of EEN. In-vivo study on the Ca^{2+} binding should also be carried out using rat or other animal models.

Although all the results in my work suggested that the random coil region of EEN may not carry any functions *in vitro*, there are possibilities that this random coil domain could play a role in the process of endocytosis *in vivo*. The full length of EEN should also be used as the object to study the functions of the random coil region on binding between EEN and proline rich domain *in vitro*.

REFERENCES

Aramaki, Y., Ogawa, K., Toh, Y., Ito, T., Akimitsu, N., Hamamoto, H., Sekimizu, K., Matsusue, K., Kono, A., Iguchi, H., Takiguchi, S. Direct interaction between metastasis-associated protein 1 and endophilin 3. FEBS Lett, 579 (17), pp. 3731-3736. 2005.

Bianca Habermann. The BAR-domain family of proteins: a case of bending and binding?. EMBO, 5, pp 250-255. 2004.

Brodin, L., Low, P., and Shupliakov, O. Sequential steps in clathrin-mediated synaptic vesicle endocytosis. Curr Opin Neurobiol, 10 (3), pp. 312-320. 2000.

Cestra, G., Castagnoli, L., Dente, L., Minenkova, O., Petrelli, A., Migone, N., Hoffmuller, U., Schneider-Mergener, J., Cesareni, G. The SH3 domains of endophilin and amphiphysin bind to the proline-rich region of synaptojanin 1 at distinct sites that display an unconventional binding specificity.J Biol Chem, 274(45), pp 32001-32007. 1999.

Chen, Y., Deng, L., Maeno-Hikichi, Y., Lai, M., Chang, S., Chen, G., Zhang, J.F. Formation of an endophilin-Ca^{2+} channel complex is critical for clathrin-mediated synaptic vesicle endocytosis. Cell, 115 (1), pp. 37-48. 2003.

Cheung, N., So, C.W., Yam, J.W., So, C.K., Poon, R.Y., Jin, D.Y., Chan, L.C., Subcellular localization of EEN/endophilin A2, a fusion partner gene in leukaemia. Biochem J, 383 (Pt 1), pp 27-35. 2004.

Fabian-Fine, R., Verstreken, P., Hiesinger, P.R., Horne, J.A., Kostyleva, R., Zhou, Y., Bellen, H.J., Meinertzhagen, I.A. Endophilin promotes a late step in endocytosis at glial invaginations in Drosophila photoreceptor terminals. J Neurosci , 23 (33), pp 10732-10744. 2003.

Farsad, K., Ringstad, N., Takei, K., Floyd, S.R., Rose K., De Camilli, P. Generation of high curvature membranes mediated by direct endophilin bilayer interactions. J Cell Biol, 155 (2), pp 193-200. 2001.

Ferreon, J.C., Volk, D.E., Luxon, B.A., Gorenstein, D.G., Hilser, V.J. Solution structure, dynamics, and thermodynamics of the native state ensemble of the Sem-5 C-terminal SH3 domain. Biochemistry, 42 (19), pp 5582-5590. 2003.

Gad, H., Ringstad, N., Low, P., Kjaerulff, O., Gustafsson, J., Wenk, M., Di Paolo, G., Nemoto, Y., Crun, J., Ellisman, M.H., De Camilli, P., Shupliakov, O., Brodin, L. Fission and uncoating of synaptic clathrin-coated vesicles are perturbed by disruption of interactions with the SH3 domain of endophilin. Neuron, 27 (2), pp. 301-312. 2000.

Goldstein, J.L., Anderson, R.G., Brown, M.S. Receptor-mediated endocytosis and the cellular uptake of low density lipoprotein. Ciba Found Symp, (92) pp 77-95. 1982.

Golovanov, A.P., Hautbergue, G.M., Wilson, S.A., Lian, L.Y. A Simple Method for Improving Protein Solubility and Long-Term Stability. J Am Chem Soc, 126(29), pp 8933-8939. 2004.

Guichet, A., Wucherpfennig, T., Dudu, V., Etter, S., Wilsch-Brauniger, M., Hellwig, A., Gonzalez-Gaitan, M., Huttner, W.B., Schmidt, A.A. Essential role of endophilin A in synaptic vesicle budding at the Drosophila neuromuscular junction. EMBO J, 21 (7), pp 1661-1672. 2002.

Habermann, B. BAR-domain family of proteins: a case of bending and binding? EMBO Rep, 5 (3), pp. 250-255. 2004.

Hill, E., van Der Kaay, J., Downes, C.P., Smythe, E. The role of dynamin and its binding partners in coated pit invagination and scission. J Cell Biol, 152 (2), pp 309-23. 2001.

Hughes, A.C., Errington, R., Fricker-Gates, R., Jones, L. Endophilin A3 forms filamentous structures that colocalise with microtubules but not with actin filaments. Brain Res Mol Brain Res, 128 (2), pp. 182-192. 2004.

Hirayama, S., Bajari, T.M., Nimpf, J., Schneider, W.J. Receptor-mediated chicken oocyte growth: differential expression of endophilin isoforms in developing follicles. Biol Reprod, 68 (5), pp 1850-1860. 2003.

Huttner, W.B., Schmidt, A. Lipids, lipid modification and lipid-protein interaction in membrane budding and fission--insights from the roles of endophilin A1 and synaptophysin in synaptic vesicle endocytosis. Curr Opin Neurobiol, 10 (5), pp 543-551. 2000.

Huttner, W.B., and Schmidt, A.A. Membrane curvature: a case of endofeelin' ... . Trends Cell Biol, 12 (4), pp. 155-158. 2002.

Jack, T. Nguyen, Christoph, W. Turck, Fred, E. Cohen, Ronald N. Zuckermann, Wendell A. Lim. Exploiting the Basis of Proline Recognition by SH3 and WW Domains: Design of N-Substituted Inhibitors. Science, vol 282, pp 2088-2092. 1998.

Karbowski, M., Jeong, S.Y., Youle, R.J. Endophilin B1 is required for the maintenance of mitochondrial morphology. J Cell Biol, 166 (7), pp. 1027-1039. 2004.

Kooijman, E.E., Chupin, V., de Kruijff, B., Burger, K.N. Modulation of membrane curvature by phosphatidic acid and lysophosphatidic acid. Traffic, 4 (3), pp 162-174. 2003.

Lua, B.L., Low, B.C. Activation of EGF receptor endocytosis and ERK1/2 signaling by BPGAP1 requires direct interaction with EEN/endophilin II and a functional RhoGAP domain. J Cell Sci, 118 (Pt 12), pp 2707-2721. 2005.

Marte, B.An. encore for kiss and run?. Nat Cell Biol, 4 (5) E123. 2002.

Micheva, K.D., Kay, B.K., McPherson, P.S. Synaptojanin forms two separate complexes in the nerve terminal Interactions with endophilin and amphiphysin. J Biol Chem, 272 (43), pp 27239-27245. 1997.

Micheva, K.D., Ramjaun, A.R., Kay, B.K., McPherson, P.S. SH3 domain-dependent interactions of endophilin with amphiphysin. FEBS Lett, 414 (2), pp 308-312. 1997.

Modregger, J., Schmidt, A.A., Ritter, B., Huttner, W.B., Plomann, M. Characterization of Endophilin B1b, a brain-specific membrane-associated lysophosphatidic acid acyl transferase with properties distinct from endophilin A1. J Biol Chem, 278 (6), pp 4160-4167. 2003.

Peter, B.J., Kent, H.M., Mills, I.G., Vallis, Y., Butler, P.J., Evans, P.R., McMahon, H.T. BAR domains as sensors of membrane curvature: the amphiphysin BAR structure. Science, 303 (5657), pp 495-499. 2004.

Reutens, A.T., Begley, C.G. Endophilin-1: a multifunctional protein. Int J Biochem Cell Biol, 34 (10), pp. 1173-1177. 2002.

Richmond, J.E., Broadie, K.S. The synaptic vesicle cycle: exocytosis and endocytosis in Drosophila and C. elegans. Curr Opin Neurobiol,12 (5), pp 499-507. 2002.

Rikhy, R., Kumar, V., Mittal, R., Krishnan, K.S. Endophilin is critically required for synapse formation and function in Drosophila melanogaster. J Neurosci, 22 (17), pp 7478-7484. 2002.

Ringstad, N., Gad, H., Low, P., Di Paolo, G., Brodin, L., Shupliakov, O., De Camilli, P. Endophilin/SH3p4 is required for the transition from early to late stages in clathrin-mediated synaptic vesicle endocytosis. Neuron, 24 (1), pp. 143-154. 1999.

Ringstad, N., Nemoto, Y., De Camilli, P. Differential expression of endophilin 1 and 2 dimers at central nervous system synapses. J Biol Chem, 276(44), pp 40424-40430. 2001.

Royle, S.J., Lagnado, L. Endocytosis at the synaptic terminal. J Physiol, 553 (Pt 2), pp 345-355. 2003.

Schmidt, A., Wolde, M., Thiele, C., Fest, W., Kratzin, H., Podtelejnikov, A.V., Witke, W., Huttner, W.B., Soling, H.D. Endophilin I mediates synaptic vesicle formation by transfer of arachidonate to lysophosphatidic acid. Nature, 401(6749), pp 133-141. 1999.

Schuske, K.R., Richmond, J.E., Matthies, D.S., Davis, W.S., Runz, S., Rube, D.A., van der Bliek, A.M., Jorgensen, E.M. Endophilin is required for synaptic vesicle endocytosis by localizing synaptojanin. Neuron,40 (4), pp 749-762. 2003.

Simpson, F., Hussain, N.K., Qualmann, B., Kelly, R.B., Kay, B.K., McPherson, P.S., Schmid, S.L. SH3-domain-containing proteins function at distinct steps in clathrin-coated vesicle formation. Nat Cell Biol, 1(2), pp 119-124. 1999.

Sittler, A., Walter, S., Wedemeyer, N., Hasenbank, R., Scherzinger, E., Eickhoff, H., Bates, G.P., Lehrach, H., Wanker, E.E. SH3GL3 associates with the Huntingtin exon 1 protein and promotes the formation of polygln-containing protein aggregates. Mol Cell, 2(4), pp 427-436. 1998.

Slepnev, V.I., and De Camilli, P. Accessory factors in clathrin-dependent synaptic vesicle endocytosis. Nat Rev Neurosci, 1 (3), pp. 161-172. 2000.

So, C.W., Caldas, C., Liu, M.M., Chen, S.J., Huang, Q.H., Gu, L.J., Sham, M.H., Wiedemann, L.M., Chan, L.C. EEN encodes for a member of a new family of proteins containing an Src homology 3 domain and is the third gene located on chromosome 19p13 that fuses to MLL in human leukemia. Proc Natl Acad Sci U S A, 94(6), pp 2563-2568. 1997.

Solomaha, E., Szeto, F.L., Yousef, M.A., Palfrey, H.C. Kinetics of Src homology 3 domain association with the proline-rich domain of dynamins: specificity, occlusion, and the effects of phosphorylation. J Biol Chem, 280 (24), pp. 23147-23156. 2005.

Song, W., Zinsmaier, K.E. Endophilin and synaptojanin hook up to promote synaptic vesicle endocytosis. Neuron, 40 (4), pp 665-667. 2003.

Stahl, P.D., Barbieri, M.A. Multivesicular bodies and multivesicular endosomes: the "ins and outs" of endosomal traffic. Sci STKE, 2002 (141), PE32. 2002.

Szaszak, M., Gaborik, Z., Turu, G., McPherson, P.S., Clark, A.J., Catt, K.J., Hunyady, L. Role of the proline-rich domain of dynamin-2 and its interactions with Src homology 3 domains during endocytosis of the AT1 angiotensin receptor. J Biol Chem, 277 (24), pp 21650-21656. 2002.

Takei, K., Slepnev, V.I., Haucke, V., De Camilli P. Functional partnership between amphiphysin and dynamin in clathrin-mediated endocytosis. Nat Cell Biol, 1(1), pp 33-39. 1999.

Tang, Y., Hu, L.A., Miller, W.E., Ringstad, N., Hall, R.A., Pitcher, J.A., DeCamilli, P., Lefkowitz, R.J. Identification of the endophilins (SH3p4/p8/p13) as novel binding partners for the beta1-adrenergic receptor. Proc Natl Acad Sci U S A, 96 (22), pp 12559-12564. 1999.

Tarricone, C., Xiao, B., Justin, N., Walker, P.A., Rittinger, K., Gamblin, S.J., Smerdon, S.J. The structural basis of Arfaptin-mediated cross-talk between Rac and Arf signalling pathways. Nature, 411(6834), pp 215-219. 2001.

Toshimichi Ikemura. Codon usage and tRNA content in unicellular organisms. Mol.Biol.Evol., 2(1), pp 13-34. 1985.

Trevaskis, J., Walder, K., Foletta, V., Kerr-Bayles, L., McMillan, J., Cooper, A., Lee, S., Bolton, K., Prior, M., Fahey, R., Whitecross, K., Morton, G.J., Schwartz, M.W., Collier, G.R. Src homology 3-domain growth factor receptor-bound 2-like (endophilin) interacting protein 1, a novel neuronal protein that regulates energy balance. Endocrinology, 146 (9), pp. 3757-3764. 2005.

Verstreken, P., Kjaerulff, O., Lloyd, T.E., Atkinson, R., Zhou, Y., Meinertzhagen, I.A., Bellen, H.J. Endophilin mutations block clathrin-mediated endocytosis but not neurotransmitter release. Cell, 109 (1), pp. 101-112. 2002.

Wang, M.Q., Kim, W., Gao, G., Torrey, T.A., Morse, H.C., De Camilli, P., Goff, S.P. Endophilins interact with Moloney murine leukemia virus Gag and modulate virion production. J Biol, 3 (1): 4. 2003.

Weissenhorn, W. Crystal structure of the endophilin-A1 BAR domain. J Mol Biol, 351 (3), pp. 653-661. 2005.

Wiejak, J., Wyroba, E. Dynamin: characteristics, mechanism of action and function. Cell Mol Biol Lett, 7 (4), pp 1073-1080. 2002.

Yam, J.W., Jin, D.Y., So, C.W., Chan, L.C. Identification and characterization of EBP, a novel EEN binding protein that inhibits Ras signaling and is recruited into the nucleus by the MLL-EEN fusion protein. Blood, 103(4), pp 1445-1453. 2004.

Zimmerberg, J., McLaughlin, S. Membrane curvature: how BAR domains bend bilayers. Curr Biol, 14 (6), pp 250-252. 2004.